

Multipolar Kondo Effect in 1S_0 - 3P_2 Mixture of ^{173}Yb Atoms

Igor Kuzmenko¹, Tetyana Kuzmenko¹, Yshai Avishai^{1,2,4} and Gyu-Boong Jo³

¹*Department of Physics,*

Ben-Gurion University of the Negev, Beer-Sheva, Israel

²*NYU-Shanghai, Pudong, Shanghai, China,*

³*Department of Physics,*

The Hong Kong University of Science and Technology,

Clear Water Bay, Kowloon, Hong Kong, China

⁴*Yukawa Institute for Theoretical Physics,*

Kyoto University, Kyoto 606-8502, Japan

Whereas in the familiar Kondo effect the exchange interaction is *dipolar*, there are systems in which the exchange interaction is *multipolar*, as has been realized in a recent experiment. Here we study multipolar Kondo effect in a Fermi gas of cold ^{173}Yb atoms. Making use of different AC polarizabilities of the electronic ground state $\text{Yb}(^1S_0)$ and the long-lived metastable state $\text{Yb}^*(^3P_2)$, it is suggested that the latter atoms can be localized and serve as a dilute concentration of magnetic impurities while the former ones remain itinerant. The exchange mechanism between the itinerant Yb and the localized Yb^* atoms is analyzed and shown to be antiferromagnetic. The quadrupole and octupole interactions act to enhance the Kondo temperature T_K that is found to be experimentally accessible. The bare exchange Hamiltonian needs to be decomposed into dipole (d), quadrupole (q) and octupole (o) interactions in order to retain its form under renormalization group (RG) analysis, in which the corresponding exchange constants (λ_d , λ_q and λ_o) flow independently. Numerical solution of the RG scaling equations reveals a few finite fixed points. Arguments are presented that the Fermi liquid fixed point at low temperature is unstable, indicating that the impurity is over-screened, which suggests a non-Fermi liquid phase. The impurity contributions to the specific heat, entropy and the magnetic susceptibility are calculated in the weak coupling regime ($T \gg T_K$), and are compared with the analogous results obtained for the standard case of dipolar exchange interaction (the $s-d$ Hamiltonian).

PACS numbers: 31.25.-v, 32.80.Pj, 72.15.Qm

I. INTRODUCTION

Background In its most elementary form, the (single channel) Kondo model describes the physics of a magnetic impurity (of spin operator \mathbf{S}), immersed in a host metal with a single continuous band of noninteracting electrons (of spin operator \mathbf{s} , with $s = \frac{1}{2}\hbar$)¹⁻⁴. The impurity and the band electrons are coupled via an antiferromagnetic exchange interaction $J\mathbf{s} \cdot \mathbf{S}$ of strength $J > 0$. The corresponding Hamiltonian H_{s-d} has an SU(2) symmetry. The Kondo model can naturally be generalized into the Coqblin-Schrieffer model whose Hamiltonian H_{C-S} has an SU(N) symmetry⁴⁻⁷. Renormalization group (RG) analysis shows that the respective low energy fixed point in either model is stable and that the corresponding fixed point Hamiltonian describes regular or singular Fermi liquid (FL), in which the impurity is fully or under screened.

A seminal paper by Nozières and Blandin (NB) back in 1980, discusses the fixed points of H_{s-d} under the assumption that a few electron channels participate in the impurity screening⁸. More precisely, suppose that by some mechanism, there are N independent electron channels contributing to screening. Then, under favourable conditions on the corresponding exchange constants, together with the (hereafter referred as NB inequality) $N > 2S$, the impurity is *over-screened*. The Hamiltonian of such over-screened Kondo system flows at low temperature to a new fixed point in which it displays a

non-Fermi liquid (NFL) behaviour. Searching for an experimental manifestation of over-screened Kondo effect in solid state systems was notoriously frustrating, but eventually it was demonstrated in a specifically designed quantum-dot system⁹.

Another route to over-screening in the Kondo effect is *single channel over-screening by large spin Fermi-sea*¹⁰. It is expected to occur when a magnetic impurity is immersed in a host Fermi-sea with a continuous band of noninteracting fermions of spin operator \mathbf{s} , with $s > \frac{1}{2}\hbar$. This system is shown to be equivalent to that with $N(s)$ independent electron channels where

$$N(s) = \frac{2}{3} s(s+1)(2s+1). \quad (1)$$

Since $N(s)$ is a cubic function of s , (for example $N(\frac{5}{2}) = 35$), the NB inequality $N > 2S$ (that is a necessary but not sufficient condition for over-screening) can easily be satisfied. While it is hard (albeit possible) to perceive its realization in solid state systems, the revelation and the possible control of a gas composed of cold fermionic atoms within a periodic optical lattice potential turned this scenario to be realistic also outside the realm of solid-state systems^{11,12}. Indeed, we have recently suggested a general framework for a pertinent experiment to test this scenario of over-screening and analyzed the conditions and parameter range for its realization¹³. It can be performed in a few laboratories that specialize in controlling cold fermionic atoms.

In both cases (multi-channel and/or large spin over screening), the corresponding Hamiltonian has an $SU(2)$ symmetry, and the exchange interaction is *dipolar*. An extension of the $SU(2)$ multi-channel over-screening scenario into over-screened multi-channel $SU(N)$ Kondo model is discussed in Ref.¹⁴.

In the present work we focus on an experimentally accessible cold atom system and examine the concept of large spin Kondo over-screening beyond $SU(2)$, in case where the exchange interaction is *multipolar*. This is motivated by a recent experiment where a multipolar Kondo effect is realized in solid state system¹². For the cold atom arena, a concrete experimental candidate system is that of fermionic alkali-earth-like isotopes such as ^{173}Yb atoms^{15–19}. The underlying idea is to localize an ^{173}Yb atom in its long lived excited $^3\text{P}_2$ state with atomic spin $F = \frac{3}{2}$, in a Fermi sea of non (or weakly)-interacting itinerant ^{173}Yb atoms in their ground state $^1\text{S}_0$ with atomic spin $I = \frac{5}{2}$. For that purpose, it should be demonstrated that an antiferromagnetic exchange interaction exists between the impurity $\text{Yb}^*(^3\text{P}_2)$ and the itinerant $\text{Yb}(^1\text{S}_0)$ atoms. Intuitively, in that case we might expect an over-screening by large spin scenario, since the angular momentum of the itinerant atoms is larger than that of the impurity atom ($I = \frac{5}{2} > F = \frac{3}{2}$). However, quantitative analysis turns out to be extremely complicated, due to several factors. First, elucidation and calculation of the exchange interaction is rather involved, and requires sophisticated multipole expansions to handle the pertinent angular momentum algebra. Second, identifying and constructing the explicit form of the exchange term is rather tedious, and, unfortunately, the pertinent Kondo Hamiltonian does not have a definite symmetry. Third, in order to identify the NFL fixed points, perturbative RG calculations within the poor-man scaling procedure must go at least up to third order and the relevant expressions are long and involve multipole summations on angular momentum quantum numbers. Finally, elucidating the NFL physics requires the use of non-perturbative techniques (Bethe ansatz or conformal field theory) which are still not developed for this class of Hamiltonians.

It is worthwhile stressing at this early stage a central point distinguishing multipolar from an $SU(2)$ over-screening resulting from our analysis: If the spin F of the impurity and the spin I of itinerant fermions satisfy the inequalities

$$F \geq 3/2, \quad I \geq 3/2, \quad N(I) > 2S,$$

the NB fixed point $j^* = 1/N(I)$ is unstable. The stable fixed points exposed here are distinct from the NB fixed point, and correspond to different NFL phases. The reason is that in the process of carrying out Schrieffer-Wolf transformations, one usually restricts oneself to second order perturbation theory. However, when quadrupole, octupole and higher exchange interactions are present, new interactions are generated within the Schrieffer-Wolf procedure. At high temperature these interactions are weaker than the lowest order (dipole) interaction. But

at low temperature, these interactions turn the NB fixed point to be unstable.

Organization: The paper is organized as follows: In section II the question of experimental realization is addressed. Specifically, we substantiate the feasibility of fabricating a system consisting of a Fermi gas of ^{173}Yb atoms in their ground state (electronic configuration $^1\text{S}_0$) and a small concentration of ^{173}Yb atoms in their long lived excited state (electronic configuration $^3\text{P}_2$) trapped in a suitably designed optical potential. The rest of the paper is devoted to theoretical analysis. The Kondo Hamiltonian H_K is derived in Sec. III. The main technical endeavours are related to the decomposition of H_K into 2^n poles components ($n = 1, 2, 3$), and the numerical estimates of the pertinent coupling constants. The single atomic energies are estimated in Sec. IV. Exchange interaction between $^{173}\text{Yb}(^1\text{S}_0)$ and $^{173}\text{Yb}^*(^3\text{P}_2)$ atoms is analyzed in section V. In Section VI the perturbative RG calculations pertaining to H_K are detailed up to second order. Although the derivation of these corrections is rather technical, we find it useful to present it within the main text because it starts from the standard diagrams of poor-man's scaling analysis, and the analysis that enables us to overcome the complexities stemming from the relevant spin algebra is quite instructive. At the end of this section we write down and solve the relevant scaling equations (up to second order). The solutions enable us to elucidate the Kondo temperature T_K , as explained in section VII. However, to find stable fixed points that are candidates for NFL behaviour, one must expand the perturbative RG calculations up to third order. These calculations are carried out in section VIII. Despite its highly technical nature, we include it in the main text, for the same reasons as for section VI. The most significant result that emerges is a list of seven possible fixed points. Yet, further stability analysis is required in order to sort out the stable ones, by linearizing the RG equations and identifying relevant and irrelevant exponents. At the end of this procedure, only three stable points are left. Analysis of the relation between the fixed points and the interaction parameters is carried out in section IX, and the claim that the infinite fixed point in the strong coupling limit is unstable is detailed in section X.

In section XI we derive (in the weak coupling regime $T > T_K$) expressions for the impurity contributions to a few thermodynamic observables related to this system, and compare them with the corresponding quantities for the standard Kondo effect based on the $s - d$ exchange Hamiltonian. These include the impurity contribution to the specific heat, entropy and magnetic susceptibility. A short summary listing our main achievements is presented in section XII. Numerous technical issues are discussed in the Appendices.

II. EXPERIMENTAL FEASIBILITY

Recent development of producing degenerate Bose and Fermi gases of alkaline-earth-like atoms has attracted a

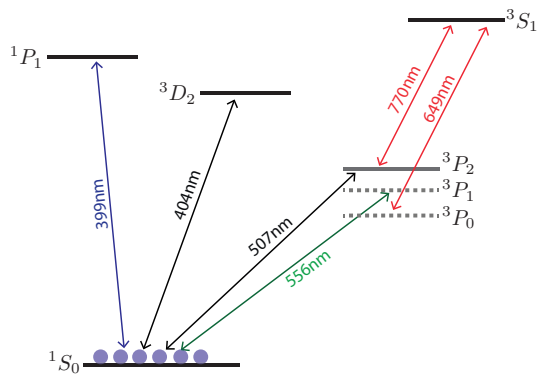


FIG. 1: (color online) The electronic level structure of ^{173}Yb atoms. A small portion of the atoms are optically pumped into the $^3\text{P}_2$ excited state via a resonant $^1\text{S}_0$ - $^3\text{P}_2$ transition or an intermediate $^1\text{S}_0$ - $^3\text{D}_2$ transition.

great deal of interests in utilizing such atoms for the study of many-body physics (in the context of quantum simulation)^{20–22} and the realization of quantum computation^{23,24}. The enlarged $\text{SU}(N)$ spin symmetry for the fermionic isotopes of alkaline-earth-like atoms expands our capability in exploring large spin physics in low dimensions²⁰ and a two-orbital Fermi gas with $\text{SU}(N)$ interactions^{21,22,25} in which the interactions can be tuned by the orbital Feshbach resonance¹⁶. In addition, a narrow optical transition between the singlet and the triplet state enables to realize a spin-orbit coupled Fermi gas with minimal heating^{26–30}, and a long-lived triplet state holds the promise in studying the Kondo effect¹⁷. It has been demonstrated that in such a systems, the Kondo temperature can be increased due to the spin-exchange interaction and the confinement-induced resonance effect¹⁸.

More concretely, making use of different AC polarizabilities of the ground state and the metastable state, the latter can be localized and serve as local moments. Kondo effect is then expected to occur due to an exchange interaction between the atoms in the ground state $^1\text{S}_0$ and the atoms in the metastable $^3\text{P}_2$ state. Such scenario, pertaining to spin-exchange interactions between $^1\text{S}_0$ and $^3\text{P}_0$ states has been explored in our previous work where it is shown to realize an $\text{SU}(6)$ Coqblin-Schrieffer model³³.

Our starting point is a degenerate Fermi gas of the ground-state ^{173}Yb atoms. Subsequently, a small portion, (a few %) of the ground state $^1\text{S}_0$ atoms will be directly excited to the $^3\text{P}_2$ level using a narrow line-width $^1\text{S}_0$ - $^3\text{P}_2$ transition at 507 nm³¹. Alternatively, the ground state atoms may be pumped into the state $^3\text{D}_2$ with a 404 nm light and then spontaneously decay to the $^3\text{P}_2$ state³². During the pumping process, a three-dimensional optical lattice potential may be applied to suppress the recoil kick in the Lamb Dicke regime.

To realize the Kondo model in a mixture of $^1\text{S}_0$ - $^3\text{P}_2$ atoms, it is critical to minimize the anisotropy of the trapping potential for the localized $^3\text{P}_2$ atoms whose

atomic polarizability α_j depends on the magnetic quantum number j ($j \equiv J_z$ with $J = 2$). Such anisotropic polarizability would lift the degeneracy of the Kondo state of localized $^3\text{P}_2$ atoms. For this reason, we propose to use the trapping light at the double-magic wavelength $\lambda_0 \simeq 546$ nm which results³² $\alpha_{|j|} = \alpha_e(\lambda_0)$ for $|j| \leq 2$. After preparing a mixture of $^1\text{S}_0$ - $^3\text{P}_2$ atoms, a three-dimensional optical lattice generated by double-magic wavelength lights is adiabatically switched on in such a way that the Fermi energy of $^1\text{S}_0$ atoms is larger than the lattice depth while the low-density $^3\text{P}_2$ atoms are localized by the lattice potential.

In the proposed experiment, ytterbium atoms in different orbitals, Yb and Yb* atoms, can be selectively detected to extract the thermodynamic quantities that will be discussed later. The Yb atom in the $^1\text{S}_0$ state are imaged using the 399 nm $^1\text{S}_0$ - $^1\text{P}_1$ transition. To image Yb* atoms, we first blast Yb atoms with 399 nm light followed by optical pumping Yb* atoms into the $^3\text{P}_1$ state with 770 nm and 649 nm lights (see Fig. 1). The pumped atoms in the $^3\text{P}_1$ state then decay to the $^1\text{S}_0$ state that can be imaged by 399 nm light³¹.

III. MULTIPOLAR KONDO HAMILTONIAN

The total Hamiltonian of the system includes the kinetic energy part H_c of the itinerant $^{173}\text{Yb}(^1\text{S}_0)$ fermion atoms, the internal excitation H_{imp} of the impurity (that is the trapped $^{173}\text{Yb}(^3\text{P}_2)$ atom), and their mutual (exchange) interaction H_K , hereafter referred to as the exchange (or Kondo) Hamiltonian. The structures of the various parts are encoded by their (1) operator content (creation, annihilation or Hubbard), (2) spin coupling geometric tensors, (3) energies of the itinerant and the impurity atoms, and (4), strength of the exchange constant. For pedagogical reasons, this section focuses on the operator content. Definition and explicit expressions for the geometrical tensors is detailed in Appendix B, while the atomic energies are defined and calculated in section IV. Finally, the estimate of the exchange constant is discussed in section V.

The expressions for H_c and H_{imp} are simple and self-evident as they are diagonal in the appropriate bases [see Eq.(3) below]. On the other hand, a proper treatment of H_K requires some care. Its expression in terms of creation, annihilation and Hubbard operators and Clebsch-Gordan coefficients [see Eq. (5) below] is relatively simple, and involves a *single bare coupling constant* λ . However, in this form, the Hamiltonian does not keep its structure under the poor-man scaling RG transformation (introduced in Sections VI and VIII). To alleviate this riddle, it is necessary to decompose the bare Hamiltonian (5) into a sum of terms with *different multi-polarities*, H_d (dipole), H_q (quadrupole), and H_o (octupole), whose strengths are determined by corresponding pre-factors λ_d , λ_q , and λ_o . Initially, the ratios $\lambda_{d,q,o}/\lambda$ are geometrical factors explicitly calculated below. However, as will be shown in Sections VI and VIII, the three coeffi-

coefficients $\lambda_{d,q,o}$ are renormalized *differently*, but the multipolar terms $H_{d,q,o}$ keep their initial form, as is required by the RG procedure. This is the reason for the multipolar decomposition. The price is that the spin algebra required for manipulating the multipolar terms is complicated.

A. The total Hamiltonian

The system's Hamiltonian reads

$$H = \underbrace{H_c + H_{\text{imp}}}_{H_0} + H_K. \quad (2)$$

Here

$$H_c = \sum_{n,i} \varepsilon_n c_{n,i}^\dagger c_{n,i}, \quad H_{\text{imp}} = \varepsilon_{\text{imp}} \sum_f X^{f,f}. \quad (3)$$

The structure of H_c is evident: The itinerant atoms are trapped in a shallow harmonic potential and form a Fermi gas. Their wave functions (determined by the harmonic quantum number n and the (nuclear) magnetic quantum number i), are derived in Appendix A. Correspondingly, $c_{n,i}$ and $c_{n,i}^\dagger$ are creation and annihilation operators of the Yb(1S_0) atoms with these prescribed quantum numbers. Expressions for the energies $\{\varepsilon_n\}$ are given in eqs. (19) [see Appendix A for further details].

The localized impurity Hamiltonian H_{imp} is expressed in terms of the Hubbard operators $X^{f=F_z, f'=F'_z}$,

$$X^{f,f'} = |F, f\rangle\langle F, f'|, \quad (4)$$

where $|F, f\rangle$ is the ket state of the localized impurity with total spin F and magnetic quantum number f . Expression for the energy ε_{imp} is given in Eq. (18).

B. The Kondo Hamiltonian

The Kondo Hamiltonian H_K describes the scattering of itinerant $^{173}\text{Yb}(^1S_0)$ and localized $^{173}\text{Yb}(^3P_2)$ atoms. Recall that the itinerant atom is in its ground state with total atomic spin $I = \frac{5}{2}$ (which is the nuclear spin since the electronic spin is zero), and the trapped atom is in the long lived excited state with its total atomic spin being $F = \frac{3}{2}$. In its bare form, the interaction between the atoms, consisting of potential scattering and exchange terms, reads³³,

$$H_K = \lambda \sum_j \sum_{f,f'} \sum_{i,i'} \sum_{n,n'} C_{J,j;I,i}^{F,f} C_{J,j;I,i'}^{F,f'} \times X^{f,f'} c_{n',i'}^\dagger c_{n,i}. \quad (5)$$

Here the total electronic spin configuration of the excited Yb(3P_2) atom is $|Jj\rangle$ with $J = 2$ and magnetic quantum number $|j| < J$, and $C_{J,j;I,i}^{F,f} = \langle JjIi|Ff\rangle$ are Clebsch-Gordan coefficients. The exchange coupling constant λ ,

a central quantity in this context, is estimated below, see eq. (24). The Kondo Hamiltonian (5) conserves the z component of the total angular momentum that is,

$$i + f' = i' + f.$$

The selection rules for the Hamiltonian (5) are,

$$\Delta f = f - f' = 0, \pm 1, \pm 2, \pm 3. \quad (6)$$

We shall now rewrite this *same Kondo Hamiltonian* as a sum of terms representing potential, dipole, quadrupole and octupole interactions,

$$H_K = H_p + H_d + H_q + H_o. \quad (7)$$

The precise expressions for these multipolar components are given in the next subsection. As will be evident from the discussion below, this form of the Hamiltonian is more complicated than its initial form (5). The reason for using the equivalent form (7) is that if one applies the RG analysis on its bare form, Eq. (5), *the structure of the Hamiltonian changes under the poor-man's scaling procedure*. In other words, in addition to the fact that the single coupling constant λ is renormalized, the Hamiltonian acquires a different structure, and that violates the spirit of the RG formalism. Consequently, we need to express the Hamiltonian in such a way that its structure is unchanged under the poor-man's scaling procedure, whereas only the coupling constants renormalize. As we shall show below, this is indeed the case once we use the form (7).

C. Multipolar terms and bare coefficients $\lambda_{d,q,o}$

The four terms in the decomposition (7) involve four exchange coefficients $\lambda_{p,d,q,o}$, each one being proportional to λ , where the respective proportionality constants are just simple geometric factors to be written down below in Eq. (12). In addition, we need to introduce three pairs of dipole, quadrupole and octupole tensors $\{F_{f,f'}^\alpha, I_{i',i}^\alpha\}$, $\{F_{f,f'}^{\alpha,\alpha'}, I_{i',i}^{\alpha',\alpha}\}$ and $\{F_{f,f'}^{\alpha,\alpha',\alpha''}, I_{i',i}^{\alpha'',\alpha',\alpha}\}$ ($F_{f,f'}^\alpha$ for the itinerant atoms and $I_{i',i}^\alpha$ for the impurity atoms), in order to manipulate the complex spin algebra. These tensors are defined in Appendix B.

We are now in a position to write down the structure of the four parts of H_K . The first term on the right hand side of eq. (7), H_p , is due to potential scattering,

$$H_p = \lambda_p \sum_f \sum_i \sum_{n,n'} X^{f,f} c_{n',i}^\dagger c_{n,i}. \quad (8)$$

The second term on the right hand side of eq. (7), H_d , is the dipole exchange interaction,

$$H_d = \lambda_d \sum_\alpha \sum_{f,f'} \sum_{i,i'} \sum_{n,n'} F_{f,f'}^\alpha I_{i',i}^\alpha X^{f,f'} c_{n',i}^\dagger c_{n,i}. \quad (9)$$

The dipole tensors $F_{f,f'}^\alpha$ and $I_{f,f'}^\alpha$ are explicitly defined in Eq. (B1) of Appendix B, and λ_d is the coupling strength

of the dipole interaction. The third term on the right hand side of eq. (7), H_q , is the quadrupole exchange interaction,

$$H_q = \lambda_q \sum_{\alpha, \alpha'} \sum_{f, f'} \sum_{i, i'} \sum_{n, n'} F_{f, f'}^{\alpha, \alpha'} I_{i', i}^{\alpha', \alpha} \times \\ \times X^{f, f'} c_{n', i'}^\dagger c_{n, i}, \quad (10)$$

where $\hat{F}_{f, f'}^{\alpha, \alpha'}$ or $\hat{I}_{f, f'}^{\alpha', \alpha}$ are explicitly defined in Eq. (B2) of Appendix B, and λ_q is the coupling strength of the quadrupole interaction. Finally, the fourth term on the right hand side of eq. (7), H_o , is the octupole interaction,

$$H_o = \lambda_o \sum_{\alpha, \alpha', \alpha''} \sum_{f, f'} \sum_{i, i'} \sum_{n, n'} F_{f, f'}^{\alpha, \alpha', \alpha''} I_{i', i}^{\alpha'', \alpha', \alpha} \times \\ \times X^{f, f'} c_{n', i'}^\dagger c_{n, i}, \quad (11)$$

where $\hat{F}_{f, f'}^{\alpha, \alpha', \alpha''}$ or $\hat{I}_{f, f'}^{\alpha', \alpha'', \alpha}$ are explicitly defined in Eq. (B4) of Appendix B, and λ_o is the coupling strength of the octupole interaction.

On the bare level (before starting the poor-man's scaling procedure), H_K is determined by a *single coupling constant* λ . Therefore, all the four coefficients λ_p , λ_d , λ_q and λ_o are simply related to λ through geometric factors. Straightforward analysis shows that the Hamiltonians (5) and (7) are identical provided,

$$\lambda_p = \frac{\lambda}{6}, \quad \lambda_d = \frac{26\lambda}{525}, \\ \lambda_q = -\frac{\lambda}{840}, \quad \lambda_o = -\frac{\lambda}{1890}. \quad (12)$$

Note that on deriving the exchange Hamiltonian (5), we neglect the spin-orbit and hyperfine interactions. It can be shown that taking into account the spin-orbit and hyperfine interactions modify the Hamiltonian (5), but leave the Hamiltonian (7), [as well as the dipole, quadrupole and octupole interactions (9), (10) and (11)] unchanged, except for slight modifications of the couplings λ_d , λ_q and λ_o . Indeed, as it is shown in Appendix G, the Hamiltonian (7) obeys spin-rotation SU(2) symmetry. The spin-orbit and hyperfine interactions satisfy the same SU(2) symmetry³⁶. As a result, the spin-orbit and hyperfine interactions cannot change the Hamiltonian (7).

IV. ATOMIC ENERGIES ε_n AND ε_{imp}

In this section the atomic energies $\{\varepsilon_n\}$ of the itinerant atoms and ε_{imp} of the impurity atom (see Eq. (3)), are computed. The main steps are: 1) Derivation of the optical potentials in which the atoms are trapped. This should be carried out separately for the ground state atoms Yb(1S_0) and the excited state atoms Yb(3P_2). 2) Solving the corresponding Schrödinger equations for the atoms in the pertinent optical potentials.

Ultra-cold Yb atoms are trapped by an optical dipole trap that is formed due to the interaction between an induced dipole moment in an atom and an external (laser) electric field $\mathbf{E}(\mathbf{r}, t)$. The oscillating electric field induces an oscillating dipole moment in the atom. Since the Yb(3P_2) atom has electronic angular momentum \mathbf{J} with $J = 2$, the atomic polarizability depends on the projection of \mathbf{J} on the direction of the electric field. Specifically, we consider an optical potential generated by an electromagnetic wave with double magic wavelength $\lambda_0 = 546$ nm, such that the polarizabilities $\alpha_g(\lambda_0)$ and $\alpha_e(\lambda_0)$ for the atoms in the ground (g) and excited (e) states do not depend on the magnetic quantum numbers (see Appendix A for details). The optical potential depends on the wave number $k_0 = \frac{2\pi}{\lambda_0}$ and the waist radius L of the laser beams. Formally, it is written as,

$$V_\nu(\mathbf{r}) = -\alpha_\nu(\lambda_0) \lim_{T \rightarrow \infty} \int_0^T |\mathbf{E}(\mathbf{r}, t)|^2 dt = \\ = V_\nu^{(\text{slow})}(\mathbf{r}) + V_\nu^{(\text{fast})}(\mathbf{r}). \quad (13)$$

Here $\nu = e$ (for the excited state 3P_2 state) and $\nu = g$ (for the ground state 1S_0). The explicit expressions for the slow and fast components read,

$$V_\nu^{(\text{slow})}(\mathbf{r}) = -V_{0, \nu} \left\{ e^{-\frac{x^2+y^2}{L^2}} + e^{-\frac{y^2+z^2}{L^2}} + e^{-\frac{z^2+x^2}{L^2}} \right\}, \\ V_\nu^{(\text{fast})}(\mathbf{r}) = -V_{1, \nu} \left\{ \cos(2k_0 x) e^{-\frac{y^2+z^2}{L^2}} + \right. \\ \left. + \cos(2k_0 y) e^{-\frac{z^2+x^2}{L^2}} + \cos(2k_0 z) e^{-\frac{x^2+y^2}{L^2}} \right\},$$

where $V_{1, \nu} \ll V_{0, \nu}$ are amplitudes of the fast-oscillating and slow-changing potentials, see eq. (A13) in Appendix A. The optical potential (13) is illustrated in Fig. 2

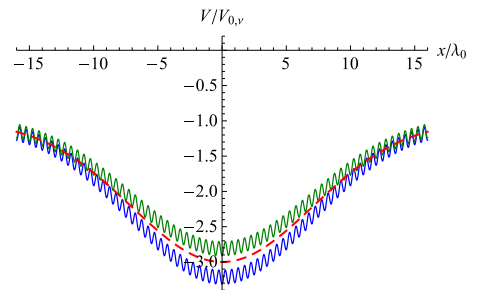


FIG. 2: (Color online) $V_\nu(x, 0, 0)$ [solid blue curve], $V_\nu(x, \lambda_0/4, \lambda_0/4)$ [solid green curve] and $V_\nu^{(\text{slow})}(x, 0, 0)$ [dashed red curve] as functions of x for $L = 10\lambda_0$ and $E_v = 0.05E_v$.

for $L = 10\lambda_0$ and $V_{1, \nu} = 0.1V_{0, \nu}$ [blue and green solid curves]. The dashed red curve show $V_\nu^{(\text{slow})}(x, 0, 0)$.

In order to find the wave functions and energies of the Yb(1S_0) and Yb(3P_2) atoms, we solve the Schrödinger equation for $\Psi^\nu(\mathbf{r})$, ($\nu=e, g$),

$$-\frac{\hbar^2}{2M} \nabla^2 \Psi^\nu(\mathbf{r}) + V_\nu(\mathbf{r}) \Psi^\nu(\mathbf{r}) = \varepsilon_\nu \Psi^\nu(\mathbf{r}). \quad (14)$$

Consider first $\Psi^e(\mathbf{r})$. We assume that the $\text{Yb}(^3\text{P}_2)$ atom is trapped by the potential $V_e^{(\text{fast})}(\mathbf{r})$. When the corresponding energy level ε_{imp} is deep enough, the wave function of the radial wave function of the bound state near the potential minimum at $\mathbf{r} = 0$ can be approximated within the harmonic potential picture as

$$\Psi^e(r) = \frac{1}{(\pi a_e^2)^{3/4}} \exp\left(-\frac{r^2}{2a_e^2}\right). \quad (15)$$

The harmonic length and frequency are,

$$k_0 a_e = \left(\frac{\mathcal{E}_0}{2V_{1,e}}\right)^{1/4}, \quad \hbar\Omega_e = 2\sqrt{2\mathcal{E}_0 V_{1,e}}, \quad (16)$$

while the recoil energy \mathcal{E}_0 is

$$\mathcal{E}_0 = \frac{\hbar^2 k_0^2}{2M}, \quad (17)$$

where M is the atomic mass. The energy ε_{imp} measured from the bottom of the well is then,

$$\varepsilon_{\text{imp}} = \frac{3}{2} \hbar\Omega_e. \quad (18)$$

Next, we consider wave functions and energy levels of $\text{Yb}(^1\text{S}_0)$ atoms. Assume that the Fermi energy ϵ_F satisfies the inequalities,

$$V_{1,g} \ll \epsilon_F \ll V_{0,g}.$$

Then for atoms with energies close to ϵ_F , we can neglect $V_g^{(\text{fast})}(\mathbf{r})$ and write

$$V_g(\mathbf{r}) \approx V_g^{(\text{slow})}(\mathbf{r}).$$

Moreover, we can approximate $V_g^{(\text{slow})}(\mathbf{r})$ by an isotropic harmonic oscillator, see appendix A for details. Atoms trapped by the isotropic harmonic oscillator potential are described by the radial quantum number $n = 0, 1, 2, \dots$, angular momentum $l = 0, 1, 2, \dots$ and projection m of the angular momentum on the axis z . Because of centrifugal barrier, only the atoms with $l = 0$ can approach the impurity and be involved in the exchange interaction with it. The energy levels of the states with $l = 0$ are

$$\varepsilon_n = \hbar\Omega_g \left(2n + \frac{3}{2}\right). \quad (19)$$

Here the harmonic length a_g and frequency Ω_g are defined as

$$\frac{a_g}{L} = \left(\frac{\mathcal{E}_L}{2V_{0,g}}\right)^{1/4}, \quad \hbar\Omega_g = 2\sqrt{2\mathcal{E}_L V_{0,g}}, \quad (20)$$

where \mathcal{E}_L is defined as,

$$\mathcal{E}_L = \frac{\hbar^2}{2ML^2}. \quad (21)$$

In the following, we assume that

$$\Omega_e \gg \Omega_g. \quad (22)$$

Within this framework, the spectrum is nearly continuous and the ytterbium atoms in the ground-state form a Fermi gas. The Fermi energy ϵ_F is such that $\epsilon_F \gg \hbar\Omega_g$, hence the Fermi gas is 3D. The density of states (DOS) pertaining to the energy dispersion (19) is

$$\rho(\epsilon) = \frac{\Theta(\epsilon)}{2\hbar\Omega_g}, \quad (23)$$

where $\Theta(\xi)$ is the Heaviside theta function equal to 0 for $\xi < 0$, 1 for $\xi > 0$ and $\frac{1}{2}$ for $\xi = 0$.

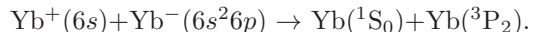
V. EXCHANGE INTERACTION

In this section, the origin of the exchange interaction between the two atoms $^{173}\text{Yb}(^3\text{P}_2)$ - $^{173}\text{Yb}(^1\text{S}_0)$ is explained, and the strength of the exchange constant λ is computed. This exchange mechanism is similar *but not identical* to the one derived within our analysis of the exchange interaction between the $^{173}\text{Yb}(^3\text{P}_0)$ - $^{173}\text{Yb}(^1\text{S}_0)$ atoms³³. The difference is that here, the total electronic spin of one of the atoms, $^{173}\text{Yb}(^3\text{P}_2)$, is not zero.

When the distance R between an itinerant atom $\text{Yb}(^1\text{S}_0)$ (whose electronic configuration is $6s^2$) and the impurity atom $\text{Yb}(^3\text{P}_2)$ (whose electronic configuration is $6s6p$) is of order R_0 (the atomic size), there is an *indirect exchange interaction* between them³³. Heuristically it is described in two steps [see Fig. 3 for illustration]: 1) The $6p$ electron tunnels from the $\text{Yb}(^3\text{P}_2)$ atom to the $\text{Yb}(^1\text{S}_0)$ atom,



As a result, we have an intermediate state with two oppositely charged ions with parallel electronic orbital angular momenta. 2) Then, one electron in a $6s$ orbital tunnels from the negatively charged ion to the $6s$ orbital of the positively charged ion.



The net outcome is that the atoms “exchange their identities” specified by their electronic quantum states: one atom transforms from the ground state to the excited state, whereas the other atom transforms from the excited state to the ground state. The detailed calculations of the pertinent exchange interaction is relegated to Appendix C (see also Ref.³³). They employ two-particle wave functions describing the motion of two atoms in the optical potential, taking into account the atom-atom interaction. For short distance between the atoms, (where the exchange interaction is essential), the two-atom wave function is determined mainly by the inter-atomic van der Waals potential³³⁻³⁵. The exchange interaction strength parameter λ is given by,

$$\lambda = \frac{\sqrt{3}k_F}{a_g^2} \Gamma^2\left(\frac{3}{2}\right) \int_{r_0}^{\infty} \mathbf{g}(R) R^2 dR. \quad (24)$$

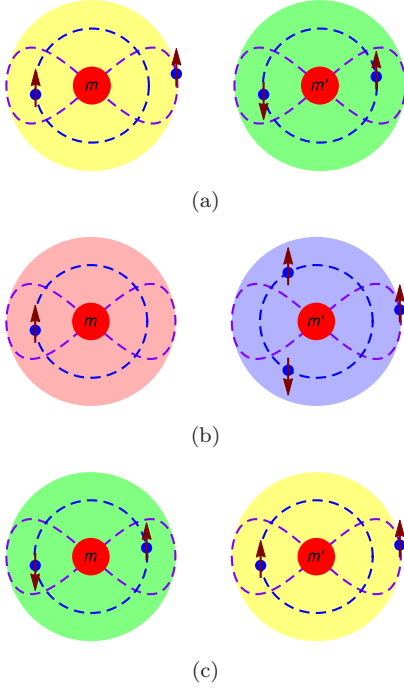


FIG. 3: (Color online) Illustration of exchange interaction between ytterbium atoms. Panel (a): Initial quantum state - the first atom is in the meta-stable state (light yellow disk) and the second one is in the ground state (light green disk); panel (b): virtual state - the first atom is positively ionized (light red disk), and the second one is negatively charged (light blue disk); panel (c): final state - the first atom is in the ground state and the other one is in the meta-stable state. For all the panels, arrows denote the electronic spin, m or m' is nuclear spin of the first or second atom.

Here

$$k_F = \frac{\sqrt{2M\epsilon_F}}{\hbar}.$$

is the Fermi wave number expressed in terms of the Fermi energy ϵ_F and the atomic mass M , while a_g is the harmonic length explicitly defined in Eq.(20). The function $g(R)$ is decomposed as,

$$g(R) = \frac{t_s(R) t_p(R)}{3 \Delta\epsilon} \mathfrak{R}(R). \quad (25)$$

[see Appendix C for details]. Here t_s and t_p are tunneling rates for the $6s$ and $6p$ electrons³³,

$$t_\mu(R) = t_\mu^{(0)} \left(\frac{R}{r_0} \right)^{\frac{2}{\beta_\mu} + \frac{1}{2}} e^{-\kappa_\mu(R-r_0)}, \quad (26)$$

where $\mu = s, p$,

$$t_s^{(0)} = 1.09 \text{ eV}, \quad t_p^{(0)} = 1.82 \text{ eV}.$$

The parameters κ_ν and β_ν are

$$\begin{aligned} \kappa_s &= 1.28122 \text{ \AA}^{-1}, & \beta_s &= 0.677994, \\ \kappa_p &= 1.00005 \text{ \AA}^{-1}, & \beta_p &= 0.529206. \end{aligned}$$

$\Delta\epsilon = \epsilon_{\text{ion}} + \epsilon_{\text{ea}} - \epsilon_x = 4.1104 \text{ eV}$ is the energy which should be paid to get positively and negatively charged ions from two neutral atoms, where $\epsilon_{\text{ion}} = 6.2542 \text{ eV}$ is the ionization energy⁴⁰, $\epsilon_{\text{ea}} = 0.3 \text{ eV}$ is the electron affinity⁴¹ and $\epsilon_x = 2.4438 \text{ eV}$ is the excitation energy of the 3P_2 state⁴⁰.

The function $\mathfrak{R}(R)$ in eq. (25) encodes the deformation of the wave function of the itinerant fermions at short distance from the impurity where the van der Waals interaction is significant³³,

$$\mathfrak{R}(R) = \frac{8c}{R^2 K(R)} \left\{ 1 + \left(\frac{a_w - \bar{a}}{\bar{a}} \right)^2 \right\}.$$

Here

$$K(R) = \frac{1}{\hbar} \sqrt{-MW(R)},$$

where $a_w = 20.9973 \text{ \AA}$, $\bar{a} = 42.9984 \text{ \AA}$ and $c = 89.9569 \text{ \AA}$. We approximate the van der Waals interaction by the Lennard-Jones potential as³⁹,

$$W(R) = -\frac{C_6}{R^6} - \frac{C_8}{R^8} + \frac{C_{12}}{R^{12}}. \quad (27)$$

Here $C_6 = 2.649 \cdot 10^3 E_h a_B^6$, $C_8 = 3.21097 \cdot 10^5 E_h a_B^8$ and $C_{12} = 1.41808 \cdot 10^9 E_h a_B^{12}$, where $E_h = 27.2114 \text{ eV}$ and $a_B = 0.529177 \text{ \AA}$. The parameter $r_0 = 3.6673 \text{ \AA}$ on the right hand side of eq. (24) is found from the condition $W(r_0) = 0$.

Anticipating the use of scaling analysis, it is useful to define the dimensionless exchange coupling constant

$$\Lambda_0 = \lambda \rho_0, \quad (28)$$

wherein $\rho_0 = \rho(\epsilon_F)$ is the density of states of the itinerant atoms at the Fermi energy, as defined in Eq. (23). Note that Λ_0 has a finite limit as $\Omega_g \rightarrow 0$ and $a_g \rightarrow \infty$. To show it, recall Eq. (24) for λ , in which a_g and Ω_g are the harmonic length and frequency explicitly defined in Eq.(20), Letting $\Omega_g \rightarrow 0$ and $a_g \rightarrow \infty$, we can write

$$\frac{1}{2\hbar\Omega_g a_g^2} = \frac{M}{4\hbar^2}, \quad (29)$$

where M is the atomic mass. Notationally, we shall write the differential scaling equations in terms of the dimensionless parameters Λ_β but keep the use of λ_β as coupling constants with dimension of energy when computing the corrections to the Hamiltonian.

VI. SECOND ORDER POOR-MAN'S SCALING ANALYSIS

In this section we derive the poor-man scaling equations to second-order in the exchange constant. This procedure is quite standard, and yet, there are important differences between the procedure applied here and that employed in the standard Kondo effect. First, we have *three coupling*

constants Λ_d, Λ_q , and Λ_o that are to be renormalized. As we see from Eqs. (32) below, these three coupling constants satisfy a set of three coupled non-linear scaling equations. Second, within the underlying representation of $SU(2)$ the number of spin projections is $2F + 1 \geq 4$, compared with $2s + 1 = 2$ in the electronic version.

Applying the poor man's scaling RG procedure to second order enables one to determine the Kondo temperature. (In order to derive scaling equations for the exchange coefficients and identifying the fixed points one has to advance to third order). For the dipolar interaction, the second order calculation procedure is straightforward and already well documented (at least for particles with spin $\frac{1}{2}$). For the multipolar exchange interactions, some technical modifications are required, as worked out below.

The "conduction" band of the (neutral) itinerant atoms is defined by their energies $\{\epsilon\}$. Before starting the RG procedure the bandwidth is D_0 . Within the RG framework, the bandwidth is narrowed in steps to be $D < D_0$ such that the energies of the atoms are constrained to be $|\epsilon - \epsilon_F| < D$ (where ϵ_F is the Fermi energy). As usual, at an intermediate stage, this conduction band is divided into three parts. The first part contains energies of particle and hole states within a reduced bandwidth $|\epsilon - \epsilon_F| < D'$, where $D' = D - \delta D$ with $\frac{\delta D}{D} \ll 1$, which are retained. The second and third parts contains energies $\{\epsilon\}$ of particle and hole states at the band edges, within narrow intervals $D' < |\epsilon - \epsilon_F| < D$. Within the RG procedure these states are to be integrated out⁴.

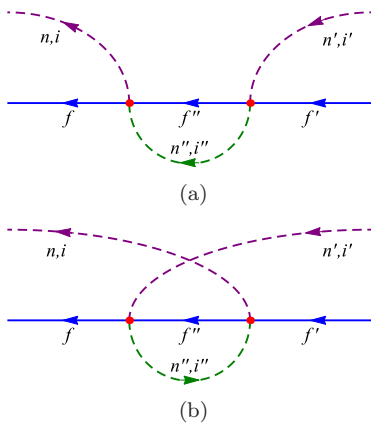


FIG. 4: (Color online) "Particle" [panel (a)] and "hole" [panel (b)] second order diagrams for the Kondo Hamiltonian (5). The solid lines correspond to the localized impurity atom, the purple dashed curves describe itinerant atoms before or after the scattering, and the green dashed curves describe itinerant atom in the virtual state near the top edge [panel (a)] or bottom edge [panel (b)] of the conduction band.

The second order corrections to the Kondo Hamiltonian are schematically illustrated in Fig. 4. Here the solid blue line describes the quantum state of the localized impurity. The dashed purple curve restricted from one side by the red dot describes itinerant atom (before or after scattering) whose energy is close to the Fermi

energy. The dashed green curves restricted by red dots from both sides describe itinerant atom in the virtual state with the energy within the interval $D' < \epsilon - \epsilon_F < D$ (as in Fig. 4(a)) or $-D < \epsilon - \epsilon_F < -D'$ (as in Fig. 4(b)). The red dots denote the Kondo Hamiltonian (7). Since H_K has three terms, the second order corrections to H_K can formally be written as,

$$\delta H_2 = \sum_{\beta, \beta'} \delta H_{\beta, \beta'}^{(2)}. \quad (30)$$

Here $\beta, \beta' = d, q, o$ for dipole, quadrupole and octupole interaction,

$$\begin{aligned} \delta H_{\beta, \beta'}^{(2)} = & \frac{1}{2} \sum_{e, e'} H_{\beta} |e\rangle \langle e| \frac{1}{\epsilon_0 - H_c} |e'\rangle \langle e'| H_{\beta'} + \\ & + \frac{1}{2} \sum_{e, e'} H_{\beta'} |e\rangle \langle e| \frac{1}{\epsilon_0 - H_c} |e'\rangle \langle e'| H_{\beta}, \end{aligned} \quad (31)$$

where $|e\rangle$ and $|e'\rangle$ are quantum states with a hole near the Fermi energy and an atom with energy in the interval $D' < \epsilon < D$, or a hole on an energy level in the interval $-D < \epsilon < -D'$ and an additional atom near the Fermi level. Recall that H_c is the Hamiltonian of itinerant atoms, see Eq. (3). Since $\delta D \ll D$, we can use the approximation,

$$\langle e| \frac{1}{\epsilon_0 - H_c} |e'\rangle \approx -\frac{1}{D} \delta_{e, e'}.$$

Explicit expressions for the operators $\delta H_{\beta, \beta'}^{(2)}$ are derived in Appendix D. Combining all the differentials $\delta H_{\beta, \beta'}^{(2)}$, we see that integrating out the virtual states near the band edges to lowest order results in a new Hamiltonian of the same form as eq. (7) but with renormalized coupling constants $\lambda_{\beta}(D) \rightarrow \lambda_{\beta}(D') = \lambda_{\beta}(D) + \delta \lambda_{\beta}$, where $\beta = d, q, o$. Consequently, we arrive at the following second order poor man's scaling equations for the dimensionless couplings $\Lambda_{\beta} = \lambda_{\beta} \rho_0$,

$$\frac{\partial \Lambda_d}{\partial \ln D} = -\Lambda_d^2 - \frac{9216}{25} \Lambda_q^2 - \frac{1469664}{25} \Lambda_o^2, \quad (32a)$$

$$\frac{\partial \Lambda_q}{\partial \ln D} = -12 \Lambda_d \Lambda_q - \frac{1458}{5} \Lambda_q \Lambda_o, \quad (32b)$$

$$\frac{\partial \Lambda_o}{\partial \ln D} = -18 \Lambda_d \Lambda_o - \frac{64}{9} \Lambda_q^2 + \frac{306}{5} \Lambda_o^2. \quad (32c)$$

Recall that $\rho_0 = \rho(0)$ is the density of states (23) of itinerant atoms at the Fermi energy ϵ_F (we set $\epsilon_F = 0$). The initial values $\Lambda_{\beta}^{(0)} = \Lambda_{\beta}(D_0)$ of the couplings Λ_{β} (where $\beta = d, q, o$) are obtained from Eq. (12) after multiplying both sides by ρ_0 , that is,

$$\Lambda_d^{(0)} = \frac{26}{525} \lambda \rho_0, \Lambda_q^{(0)} = -\frac{1}{840} \lambda \rho_0, \Lambda_o^{(0)} = -\frac{1}{1890} \lambda \rho_0. \quad (33)$$

Note that when the initial values of Λ_q and Λ_o are zero, the right hand sides of eqs. (32b) and (32c) vanish and

the set of equations (32) reduces to the standard scaling equation for the s-d Kondo model⁴,

$$\frac{\partial \Lambda_d}{\partial \ln D} = -\Lambda_d^2. \quad (34)$$

Finally, it should be noted that the scaling procedure is carried out until the effective bandwidth D essentially exceeds $\hbar\Omega_g$ and T_K [where T_K is the Kondo temperature defined below]. In the following, we assume that $\hbar\Omega_g < T_K$, and therefore the Kondo temperature is the infrared cutoff parameter of our theory.

In the next section we elucidate the effect of the quadrupole and octupole interactions on the scaling invariant of the RG equations, that is, the Kondo temperature⁴ and show that it is rather significant.

VII. KONDO TEMPERATURE

In this section, the Kondo temperature is calculated and numerically estimated, based on the results of the previous section. The important conclusion from this analysis is that this central energy scale is within an experimental reach.

The Kondo temperature is defined as the value of D for which the running coupling constants $\Lambda_\beta(D)$ diverge ($\beta = d, q, o$). To elucidate it, we solve the set of equations (32) numerically for different initial values $\Lambda_\beta^{(0)}$. Using eq. (33), it is possible to express $\Lambda_q^{(0)}$ and $\Lambda_o^{(0)}$ in terms of $\Lambda_d^{(0)}$. Then the Kondo temperature becomes a function of a single parameter, that is $\Lambda_d^{(0)}$. The results of these numerical calculations for the Kondo temperature are displayed in Fig. 5, (solid curve). In fact, T_K can be approximated by the following expression,

$$T_K = D_0 \exp\left(-\frac{1}{A\Lambda_d^{(0)}}\right), \quad A = 13.9594. \quad (35)$$

This approximation (35) for T_K is compared with the numerical results as displayed in Fig. 5, (dashed curve). It is clear that the approximation (35) is excellent. Note

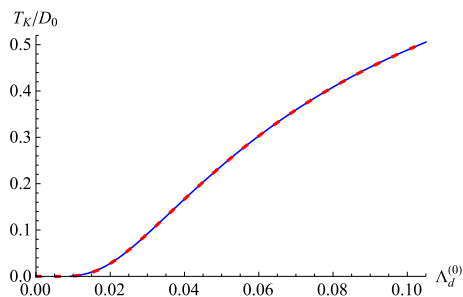


FIG. 5: (Color online) Kondo temperature calculated numerically from the set of equations (32) [solid blue curve] and the approximation (35) [dashed red curve].

that the scaling equation (34) yields the following expres-

sions for the Kondo temperature,

$$T_K^{(d)} = D_0 \exp\left(-\frac{1}{\Lambda_d^{(0)}}\right). \quad (36)$$

The factor $A \gg 1$ in eq. (35) indicates that the quadrupole and octupole interactions are important and act to enhance T_K . Numerical calculations yield $0.03D_0 < T_K < 0.1D_0$ for $400 \text{ nK} < T_F < 1000 \text{ nK}$. When $D_0 = 300 \text{ nK}$, the Kondo temperature is $9 \text{ nK} < T_K < 30 \text{ nK}$. With today's cooling techniques, it is concluded that T_K is experimentally accessible so that the multipolar Kondo effect can be measured.

VIII. THIRD ORDER POOR-MAN'S SCALING ANALYSIS

A necessary (but not sufficient) condition for arriving at a novel fixed point (at which over-screening occurs), is to check that such point is a *finite solution of third order scaling equations*. Derivation and solutions of these equations is carried out in this section. As expected, the calculations are rather involved due to the occurrence of higher multipoles, third order diagrams and spin $s > \frac{1}{2}$. Nevertheless, these cumbersome calculations should not mask the important physical consequence exposed here: There are three candidates for stable finite fixed points P_4, P_5 and P_7 (see below), that correspond to non-Fermi liquid ground-states.

In order to derive the third order correction to the poor-man's scaling equations (32), we need to consider the second order correction to the energy of the system, as encoded in the self energy diagrams shown in Fig. 6, as well as the third order vertex diagrams shown in Fig. 7 (see Ref.⁴). These diagrams are considered below each one in its turn.

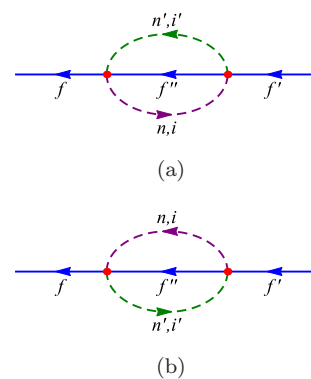


FIG. 6: (Color online) “Particle” [panel (a)] and “hole” [panel (b)] second order self energy diagrams. The solid lines correspond to the localized impurity atom, the purple dashed curves restricted by the vertex from one side describe itinerant atoms before or after the scattering, the purple dashed curves restricted by vertex from both sides describe itinerant atoms in the virtual state in the reduced energy band and the green dashed curves describe itinerant atom in the virtual state near the top edge [panel (a)] or bottom edge [panel (b)] of the conduction band.

A. Second Order Self Energy Diagrams

Second order corrections to the self energy are illustrated by the diagrams displayed in Fig. 6 and calculated in Appendix E. Taking into account eqs. (E5), (E8) and (E10), we get

$$\delta E = -\frac{\delta D}{D} E \left\{ \frac{525}{4} \Lambda_d^2 + 13440 \Lambda_q^2 + 3306744 \Lambda_o^2 \right\}. \quad (37)$$

B. Third Order Vertex Diagrams

The third order contributions to the scaling equations are given by diagrams in Fig. 7. The corresponding correction to the Kondo Hamiltonian is decomposed as,

$$\delta H_3 = \sum_{\beta, \beta'} \delta H_{\beta', \beta, \beta'}^{(3)}, \quad (38)$$

where $\beta, \beta' = d, q, o$ for the dipole, quadrupole and octupole interactions. Explicitly, we get,

$$\begin{aligned} \delta H_{\beta', \beta, \beta'}^{(3)} &= \frac{\lambda_\beta \lambda_{\beta'}^2}{D^2} \sum_{\vec{\alpha}_\beta, \vec{\alpha}_{\beta'}, \vec{\alpha}'_{\beta'}} \sum_{f, f'} \left(\hat{F}^{\vec{\alpha}_{\beta'}} \hat{F}^{\vec{\alpha}_\beta} \hat{F}^{\vec{\alpha}'_{\beta'}} \right)_{f, f'} \times \\ &\times X^{f, f'} \sum_{i, i'} \sum_{n, n'} I_{i, i'}^{\vec{\alpha}_\beta} c_{n, i}^\dagger c_{n', i'} \times \\ &\times \text{Tr} \left(\hat{I}^{\vec{\alpha}_{\beta'}} \hat{I}^{\vec{\alpha}'_{\beta'}} \right) 2\rho_0^2 D \delta D. \end{aligned} \quad (39)$$

Recall that $\hat{F}^{\vec{\alpha}_\beta}$ or $\hat{I}^{\vec{\alpha}_\beta}$ are dipole ($\beta = d$), quadrupole ($\beta = q$) and octupole ($\beta = o$) tensors for a localized impurity or itinerant atoms, $\vec{\alpha}_d \equiv \alpha$, $\vec{\alpha}_q \equiv (\alpha, \alpha')$ and $\vec{\alpha}_o \equiv (\alpha, \alpha', \alpha'')$, where α 's are Cartesian indices [see eqs. (B1), (B2) and (B4)].

Explicit expressions for the operators $\delta H_{\beta', \beta, \beta'}^{(3)}$ are derived in Appendix F. It is shown there that $\tilde{H}_K + \delta H_2 + \delta H_3$ has the *same form* as H_K , albeit with proper corrections to the coupling constants $\lambda_\beta + \delta \lambda_\beta$. Therefore we conclude that inclusion of δH_3 does not change the structure of the initial Kondo Hamiltonian *in its decomposed form* Eq.(7), but it causes a renormalization of the coupling constants $\lambda_{\beta=d, q, o}$.

C. Third Order Poor Man's Scaling Equations

The effective Hamiltonian (which includes energy and vertex renormalization) depends on the energy⁴ which is determined through the Schrödinger equation

$$H\Psi = E\Psi,$$

and this dependence is given by⁴

$$\tilde{H}_{\text{eff}}(E) = \tilde{H}_{\text{eff}}(0) - ES,$$

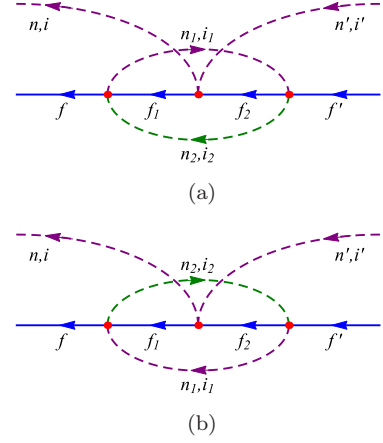


FIG. 7: (Color online) “Particle” [panel (a)] and “hole” [panel (b)] third order diagrams for the Kondo Hamiltonian (5). The solid lines correspond to the localized impurity atom, the purple dashed curves restricted by the vertex from one side describe itinerant atoms before or after the scattering, the purple dashed curves restricted by vertex from both sides describe itinerant atoms in the virtual state in the reduced energy band and the green dashed curves describe itinerant atom in the virtual state near the top edge [panel (a)] or bottom edge [panel (b)] of the conduction band.

where the parameter $S = \delta E/E$ does not depend on E , (see eq. (37)), and

$$\tilde{H}_{\text{eff}}(0) = H_K + \delta H_2 + \delta H_3, \quad (40)$$

in which δH_2 and δH_3 are given by eqs. (30) and (38). In order to get an effective Hamiltonian, we solve the (implicit) secular equation,

$$|\tilde{H}_{\text{eff}}(E) - E| = 0,$$

(where $|A|$ denotes the determinant of the square matrix A) which leads to

$$|\tilde{H}_{\text{eff}}(0) - (1 + S)E| = 0.$$

This equation yields an energy-independent effective Hamiltonian,

$$H_{\text{eff}} = (1 + S)^{-1/2} \tilde{H}_{\text{eff}}(0) (1 + S)^{-1/2}.$$

Taking into account that $S \sim \lambda^2$ [see eq. (37)] and keeping the terms up to λ^3 , we can write H_{eff} as,

$$H_{\text{eff}} = H_K + \delta H_2 + \delta \tilde{H}_3, \quad (41)$$

where

$$\delta \tilde{H}_3 = \delta H_3 + S H_K. \quad (42)$$

Employing the results of subsections VIII A and VIII B, we can see that the operator $\delta \tilde{H}_3$ has the same form as the Hamiltonian H_K , (see eq. (7) and the equations below it). Therefore, it gives rise to renormalization of the coupling constants λ_β . The third order poor-man

scaling equations for the dimensionless couplings Λ_β are then,

$$\frac{\partial \Lambda_\beta}{\partial \ln D} = \mathfrak{F}_\beta(\Lambda_d, \Lambda_q, \Lambda_o), \quad (\beta = d, q, o). \quad (43)$$

The functions $\mathfrak{F}_{d,q,o}$ on the RHS are,

$$\begin{aligned} \mathfrak{F}_d = & -\Lambda_d^2 - \frac{9216}{25} \Lambda_q^2 - \frac{1469664}{25} \Lambda_o^2 + 35 \Lambda_d^3 + \\ & + 12096 \Lambda_d \Lambda_q^2 + \frac{21493836}{5} \Lambda_d \Lambda_o^2, \end{aligned} \quad (44a)$$

$$\begin{aligned} \mathfrak{F}_q = & -12 \Lambda_d \Lambda_q - \frac{1458}{5} \Lambda_q \Lambda_o + \frac{945}{8} \Lambda_q \Lambda_d^2 + \\ & + 17472 \Lambda_q^3 + \frac{15380348}{5} \Lambda_q \Lambda_o^2, \end{aligned} \quad (44b)$$

$$\begin{aligned} \mathfrak{F}_o = & -18 \Lambda_d \Lambda_o - \frac{64}{9} \Lambda_q^2 + \frac{306}{5} \Lambda_o^2 + \frac{1365}{8} \Lambda_o \Lambda_d^2 + \\ & + 12096 \Lambda_o \Lambda_q^2 + \frac{16769916}{5} \Lambda_o^3. \end{aligned} \quad (44c)$$

The symmetry of the scaling equations (43) should be noted: \mathfrak{F}_d and \mathfrak{F}_o are even with respect to the inversion transformation $\Lambda_q \rightarrow -\Lambda_q$, whereas \mathfrak{F}_q is odd. Therefore we can safely conclude that the scaling equations (43) are invariant with respect to the inversion $\Lambda_q \rightarrow -\Lambda_q$. The fixed points of the scaling equations (43) are found from the conditions, $\mathfrak{F}_{d,q,o} = 0$. Numerical solution of the last set of equations yields seven fixed points in 3D parameter space, $P_n = (\Lambda_d^{(n)}, \Lambda_q^{(n)}, \Lambda_o^{(n)})$, $n = 1, 2, \dots, 7$:

$$P_1 = (0.0285714, 0, 0), \quad (45a)$$

$$P_2 = (0.0193713, -0.00192056, -0.000158648), \quad (45b)$$

$$P_3 = (0.0193713, 0.00192056, -0.000158648), \quad (45c)$$

$$P_4 = (0.0147126, -0.00101842, 0.00026056), \quad (45d)$$

$$P_5 = (0.0140075, 0, -0.000264616), \quad (45e)$$

$$P_6 = (0.0140587, 0, 0.000246764), \quad (45f)$$

$$P_7 = (0.0147126, 0.00101842, 0.00026056). \quad (45g)$$

There is one more fixed point, $P_0 = (0, 0, 0)$, but it is unstable, see scaling equations (32).

The scaling pattern of the parameters Λ_β ($\beta = d, q, o$) depends on the initial values of the parameters. The initial values of Λ_β are given by eq. (33) [see also eq. (12)]. They consist of the dimensionless parameter $\lambda\theta_0$ which is calculated from a microscopic model of interaction of a Yb atom in the 1S_0 state with an Yb atom in the 3P_2 state, see eq. (24). It is seen that Λ_d is positive, whereas Λ_q and Λ_o are negative.

To proceed further, it is necessary to carry out stability analysis and study the scaling of Λ_d , Λ_q and Λ_o near the fixed points $P_n = (\Lambda_d^{(n)}, \Lambda_q^{(n)}, \Lambda_o^{(n)})$. For this purpose we introduce the variables x_d , x_q and x_o ,

$$\Lambda_d = \Lambda_d^{(n)} + x_d,$$

$$\Lambda_q = \Lambda_q^{(n)} + x_q,$$

$$\Lambda_o = \Lambda_o^{(n)} + x_o,$$

and assume that x_β [$\beta = d, q, o$] are small. Expanding the functions \mathfrak{F}_β , eq. (44), in x_β to first (linear) order we get,

$$\mathfrak{F}_\beta(\Lambda_d, \Lambda_q, \Lambda_o) = \sum_{\beta'=d,q,o} A_{\beta,\beta'} x_{\beta'} + O(x^2),$$

where

$$A_{\beta,\beta'} = \left(\frac{\partial \mathfrak{F}_\beta}{\partial \Lambda_{\beta'}} \right)_{P_n},$$

the derivative is taken at the fixed point P_n . Thereby we get a set of linear differential equations for x_β ,

$$\frac{\partial x_d}{\partial \ln D} = A_{d,d} x_d + A_{d,q} x_q + A_{d,o} x_o, \quad (46a)$$

$$\frac{\partial x_q}{\partial \ln D} = A_{q,d} x_d + A_{q,q} x_q + A_{q,o} x_o, \quad (46b)$$

$$\frac{\partial x_o}{\partial \ln D} = A_{o,d} x_d + A_{o,q} x_q + A_{o,o} x_o. \quad (46c)$$

The solution of the set of equations (46) is of the form,

$$x_\beta \propto D^\gamma,$$

where the Lyapunov exponent γ is an eigenvalue of the set of equations (46). The set of three linear equations has, as a rule, three eigenvalues. A fixed point P_n is stable when all x_β tend to zero as D tends to zero. This occurs when all γ 's are positive. Accordingly, we now write down the numerical values of the triples $(\gamma_1, \gamma_2, \gamma_3)$ for each one of the fixed points $P_1 - P_7$ in its turn and determine its stability (s=stable, u=unstable).

$$P_1 : (\gamma_1, \gamma_2, \gamma_3) = (0.0285714, -0.246429, -0.375) \Rightarrow u.$$

$$P_2 : (\gamma_1, \gamma_2, \gamma_3) = (0.341287, -0.228946, 0.163813) \Rightarrow u.$$

$$P_3 : (\gamma_1, \gamma_2, \gamma_3) = (0.341287, -0.228946, 0.163813) \Rightarrow u.$$

$$P_4 : (\gamma_1, \gamma_2, \gamma_3) = (0.44974, 0.320668, 0.0632014) \Rightarrow s.$$

$$P_5 : (\gamma_1, \gamma_2, \gamma_3) = (0.434777, 0.14764, 0.14764) \Rightarrow s.$$

$$P_6 : (\gamma_1, \gamma_2, \gamma_3) = (0.40609, 0.271873, -0.0300051) \Rightarrow u.$$

$$P_7 : (\gamma_1, \gamma_2, \gamma_3) = (0.44974, 0.320668, 0.0632014) \Rightarrow s.$$

Note that P_1 is the NB fixed point, that in this case is unstable. Accordingly, only P_4 , P_5 and P_7 are stable. Elucidation of these three stable fixed points such that the corresponding fixed point Hamiltonians display non-Fermi liquid behavior (see section X) is one of the central results of the present work.

IX. ANALYSIS OF THE SCALING EQUATIONS

Analysis of the flow pattern for the system of three coupled non-linear scaling equations constructed above is rather rich and complicated. To some extent, in Figs. 8 and 9, we work out the analogue of the celebrated Anderson-Yuval equations (derived for the anisotropic Kondo effect), as adapted for the present model. Unlike the former case, however, where the fixed points are at infinity, the present analysis leads to the occurrence of finite fixed points.

Let us inspect the scaling equations (43) in some details. Note that when $\Lambda_q = \Lambda_o = 0$, then the s-d model is recovered as a special case, and scaling of Λ_d depends on the sign of $\Lambda_d^{(0)}$. For $\Lambda_d^{(0)} > 0$ $\Lambda_d(D)$ flows towards the Nosièr-Blandin fixed point P_1 , eq. (45a) indicating an over-screened Kondo effect. When $\Lambda_d^{(0)} < 0$, $\Lambda_d(D)$ flows towards zero which means that there is no Kondo effect. When $\Lambda_q^{(0)}$ and/or $\Lambda_o^{(0)}$ are non-zero, the scenario is more complicated. In order to analyze scaling, we consider the following equations,

$$\frac{\partial \Lambda_q}{\partial \Lambda_d} = \frac{\mathfrak{F}_q(\Lambda_d, \Lambda_q, \Lambda_o)}{\mathfrak{F}_d(\Lambda_d, \Lambda_q, \Lambda_o)}, \quad (47a)$$

$$\frac{\partial \Lambda_o}{\partial \Lambda_d} = \frac{\mathfrak{F}_o(\Lambda_d, \Lambda_q, \Lambda_o)}{\mathfrak{F}_d(\Lambda_d, \Lambda_q, \Lambda_o)}, \quad (47b)$$

where $\mathfrak{F}_{d,q,o}$ are given by eq. (44). Solving the set of equations (47), we get Λ_q and Λ_o as functions of Λ_d . Numerical solution of the set of equations is illustrated in Figs. 8 and 9, and implies that there are several scaling regimes as follows:

- All the running coupling constants Λ_β flow to zero as $D \rightarrow 0$, hence there is no Kondo effect.
- The running coupling constants Λ_β flow to one of the stable fixed points. In this case, Kondo effect realizes.

At this stage it should be determined for which values of the coupling constants $\Lambda_\beta^{(0)}$ there is Kondo effect, and for which ones there is not. Our numerical analysis shows that when $\Lambda_d > 0$, Kondo effect *always exists* (see Fig. 9). Therefore it is left to investigate the case $\Lambda_d^{(0)} < 0$. The result of our numerical calculations for this case is shown in Fig. 8.

We are now in a position to analyze the different scaling regimes displayed in this figure. When the ef-

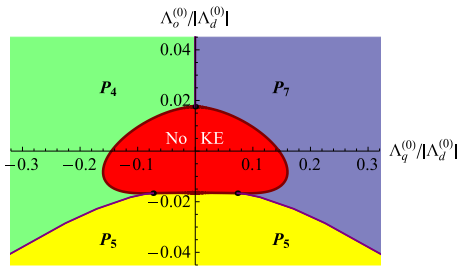


FIG. 8: (Color online) Scaling of Λ_d , Λ_q and Λ_o for $\Lambda_d^{(0)} = -0.00105$ and different values of $\Lambda_q^{(0)}$ and $\Lambda_o^{(0)}$. The red area: all Λ 's flow to zero and there is no Kondo effect. Green area: Λ 's flow to the fixed point P_4 . Yellow area: Λ 's flow to the fixed point P_5 . Blue area: Λ 's flow to the fixed point P_7 .

fective bandwidth decreases, the coupling Λ_d increases from its negative initial value and tends to 0. At this stage, it is important to determine whether $|\Lambda_q(D)|$ and $|\Lambda_o(D)|$ decrease faster or slower than $|\Lambda_d(D)|$. In other

words, we should consider the dimensionless parameters \mathcal{K}_β ($\beta = d, q, o$), defined as,

$$\mathcal{K}_\beta = \frac{\partial \ln |\Lambda_\beta(D_0)|}{\partial \ln D_0}.$$

(For $\Lambda_d < 0$, all \mathcal{K}_β are positive). When $\mathcal{K}_d < \mathcal{K}_{q,o}$, the couplings $\Lambda_{q,o}$ vanish faster than Λ_d . As a result, the Kondo Hamiltonian renormalizes towards the s-d model Hamiltonian with ferromagnetic coupling $\Lambda_d(D)$. This coupling flows towards zero when D vanishes. This is the case when Λ_β are in the red area in Fig. 8 (see also dark red arrowed curves in Fig. 9).

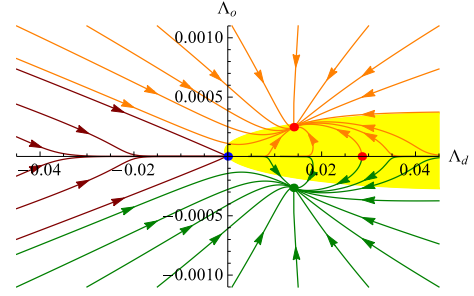


FIG. 9: (Color online) Scaling of Λ_d and Λ_o for $\Lambda_q = 0$. Dark red arrowed lines: the couplings rescale to zero. Green lines: the couplings renormalize towards the stable fixed point P_5 , eq. (45e). Orange lines: the couplings renormalize towards the saddle fixed point P_6 , eq. (45f). When Λ_q is very small but not zero, the couplings renormalize towards the fixed points P_4 or P_7 , eqs. (45d) or (45g) depending on whether the initial value of Λ_q is negative or positive.

When $\mathcal{K}_q < \mathcal{K}_d$ and/or $\mathcal{K}_o < \mathcal{K}_d$, then Λ_d vanishes when Λ_q and/or Λ_o assume finite values. At this point, Λ_β continues to flow [see eqs. (43) and (44)]. Λ_d , for example, changes its sign and the couplings Λ_β flow towards one of the fixed points, P_4 , P_5 or P_7 (green, yellow and blue areas in Fig. 8). Note that quadrupole and octupole interaction give rise to exotic property of the Kondo effect: *The effective dipole coupling $\Lambda_d(T)$ as a function of temperature turns from ferromagnetic at high temperature to antiferromagnetic at low temperature*. This property is shown in Fig. 9, see orange and green arrowed curves.

It should be noted that when $\Lambda_q = 0$, the function $\mathfrak{F}_q = 0$ [see eq. (44b)]. Therefore, when $\Lambda_q^{(0)} = 0$, then $\Lambda_q(D) = 0$ for any $D < D_0$. Consider renormalization of Λ_d and Λ_o in the plane $\Lambda_q = 0$. Numerical solution of eq. (47b) for $\Lambda_q(0) = 0$ is displayed in Fig. 9. It is seen that the couplings flow to one of the fixed points, P_0 , P_5 or P_6 , eq. (45). In order to check stability of the solution, we apply the Lyapunov method for stability. For this purpose, we consider the scaling equation for $\Lambda_q(D)$,

$$\frac{\partial \Lambda_q}{\partial \ln D} = \mathfrak{F}_q(\Lambda_d, \Lambda_q, \Lambda_o),$$

with infinitesimal initial condition $\Lambda_q^{(0)}$. Keeping just the linear power of Λ_q on the right hand side of the last

equation we may write,

$$\frac{\partial \Lambda_q}{\partial \ln D} = \Lambda_q \mathcal{A}_q(\Lambda_d, \Lambda_o), \quad (48)$$

where

$$\mathcal{A}_q(\Lambda_d, \Lambda_o) = \lim_{\Lambda_q \rightarrow 0} \left(\frac{\partial \mathfrak{F}_q(\Lambda_d, \Lambda_q, \Lambda_o)}{\partial \Lambda_q} \right).$$

The solution of eq. (48) is,

$$\frac{\Lambda_q(D)}{\Lambda_q^{(0)}} = \exp \left\{ - \int_D^{D_0} \mathcal{A}_q(\Lambda_d(D'), \Lambda_o(D')) \frac{dD'}{D'} \right\}. \quad (49)$$

Note that when D vanishes, Λ_d and Λ_o flow to one of the fixed points (45), where \mathcal{A}_q takes a finite value. In this case the integral on the right hand side of eq. (49) diverges. Thus, we conclude that when \mathcal{A}_q is positive along all the scaling trajectories of $\Lambda_d(D)$ and $\Lambda_o(D)$, then $\Lambda_q(D)$ flows to zero, and the solution displayed in Fig. 9 is stable. When \mathcal{A}_q is negative, then $\Lambda_q(D)$ flows away from zero, and the solution displayed in Fig. 9 is unstable. The interval of Λ_d and Λ_o where the solution displayed in Fig. 9 is unstable is marked by yellow.

Finally, we just state our result pertaining to scaling of the couplings satisfying the initial conditions (33). Numerical analysis shows that for any positive λ , the couplings flow towards the fixed point P_5 .

X. THE STRONG COUPLING REGIME

It is expected that the physics of an over-screened Kondo effect is exposed mainly in the strong coupling regime. Limiting one to the weak coupling regime turns it difficult to determine whether the pertinent Kondo physics at the stable points is that of over-screening or under screening. Thus, after the candidates for stable fixed points are identified, it is necessary to elucidate the ground-state wave functions at these points. The reason is at least two-fold. First, it is required in order to evaluate physical observables at low temperatures $T < T_K$. Second, it is essential to determine whether the strong coupling fixed point is unstable, so that according to NB analysis, there is a stable finite fixed point, and over-screening does occur. This task is carried out below, using variational wave functions. It is then found that the nature of the system (whether there is or there is no over-screening) depends on the initial values of the bare constants λ_d , λ_q and λ_o . Similar (albeit simpler) situation is encountered in the two-channel Kondo effect based on the $s-d$ Hamiltonian.

The variational method is an appropriate tool for that purpose, as it is not based on perturbation theory. It can be shown that the minimal energy can be reached when the number of atoms over the fully occupied Fermi sphere is $\mathcal{N} = I + \frac{1}{2}$. For $I = \frac{5}{2}$, $\mathcal{N} = 3$. Such a three particle wave function is encoded by the spin S of the three atoms.

The maximal value of the spin is $S = \frac{9}{2}$. This value is obtained as follows: according to the Pauli principle, the magnetic quantum numbers satisfy the inequalities $i_1 \neq i_2$, $i_2 \neq i_3$ and $i_3 \neq i_1$. Therefore the maximal magnetic quantum number of the three atoms is $S = \frac{9}{2}$.

A simple form of a variational wave function is,

$$|\Sigma, m\rangle = \sum_{f, \{i\}_3, \{n\}_3} C_{S, s; F, f}^{\Sigma, m} \psi_{\Sigma}(n_1) \psi_{\Sigma}(n_2) \psi_{\Sigma}(n_3) \times \\ \times C_{I, i_1; I, i_2; I, i_3}^{S, s} c_{n_1, i_1}^{\dagger} c_{n_2, i_2}^{\dagger} c_{n_3, i_3}^{\dagger} |f; \Omega\rangle, \quad (50)$$

where $|f; \Omega\rangle$ describes an impurity with magnetic quantum number f and a Fermi sea at Fermi energy ϵ_F . The Clebsch-Gordan coefficients, $C_{S, s; F, f}^{\Sigma, m}$ entail the restriction $\Sigma = S + F, S + F - 1, S + F - 2, \dots, S - F$ on the total angular momentum of the four atom system (three itinerant and one impurity). The symbols $C_{I, i_1; I, i_2; I, i_3}^{S, s}$ are the so called three particle Clebsch-Gordan coefficients. Here we use the fact that H_d , H_q and H_o commute with each other (see Appendix G for details), and therefore the four-atomic orbital angular momentum Σ is a good quantum number.

In order to find the components $\psi_{\Sigma}(n)$, we write down the Schrödinger equation,

$$H|\Sigma, m\rangle = \varepsilon|\Sigma, m\rangle,$$

and that yields the algebraic eigenvalue problem,

$$(\varepsilon_n - \varepsilon)\psi_{\Sigma}(n) + g_{\Sigma} \sum_{n'} \Theta(\varepsilon_{n'} - \varepsilon_F)\psi_{\Sigma}(n') = 0. \quad (51)$$

Here

$$g_{\Sigma} = \left\{ \lambda_d \mathcal{D}_{\Sigma} + \lambda_q \mathcal{Q}_{\Sigma} + \lambda_o \mathcal{O}_{\Sigma} \right\} \frac{k_F}{a_g^2}, \quad (52)$$

where

$$\mathcal{D}_{\Sigma} = \frac{1}{2} \left\{ \Sigma(\Sigma + 1) - F(F + 1) - I(I + 1) \right\}, \\ \mathcal{Q}_{\Sigma} = 4 \mathcal{D}_{\Sigma}^2 + 2 \mathcal{D}_{\Sigma} - \frac{4}{3} F(F + 1) S(S + 1), \\ \mathcal{O}_{\Sigma} = 36 \mathcal{D}_{\Sigma}^3 + 72 \mathcal{D}_{\Sigma}^2 + 12 \mathcal{D}_{\Sigma} - \\ - \frac{12}{5} (3S(S + 1) - 1) (2F(F + 1) - 1) \mathcal{D}_{\Sigma} - \\ - 18 S(S + 1) F(F + 1).$$

The solution of eq. (51) is,

$$\psi_{\Sigma}(n) = \frac{A_{\Sigma}}{\varepsilon_{\Sigma} - \varepsilon_n},$$

where A_{Σ} is a normalization constant. The energy ε_{Σ} can be found from the equation,

$$g_{\Sigma} \sum_n \frac{\Theta(\varepsilon_n - \varepsilon_F)}{\varepsilon_{\Sigma} - \varepsilon_n} + 1 = 0. \quad (53)$$

We are interested in the energies ε_{Σ} which are below the Fermi energy ε_F . This is the case when $g_{\Sigma} < 0$. Introducing the density of states, we can write,

$$\varepsilon_{\Sigma} - \varepsilon_F = D_0 \exp \left(- \frac{1}{|g_L| \rho_0} \right).$$

The energy of the ground state is found as

$$\varepsilon_{\text{gs}} = \min_{\Sigma} \varepsilon_{\Sigma}.$$

Thus, the problem of finding the ground state reduces to that of finding a minimum of g_{Σ} . In order to check whether the magnetic impurity is over-screened or under-screened, we consider the operator

$$(\mathbf{\Sigma} \cdot \mathbf{F}) = \frac{1}{2} \{ \Sigma(\Sigma + 1) + F(F + 1) - S(S + 1) \}. \quad (54)$$

When $(\mathbf{\Sigma} \cdot \mathbf{F}) < 0$, there is over-screened Kondo effect. Using eq. (54), the inequality becomes,

$$\Sigma(\Sigma + 1) + F(F + 1) - S(S + 1) < 0. \quad (55)$$

For $S = \frac{9}{2}$ and $F = \frac{3}{2}$, the inequality (55) is fulfilled whenever $\Sigma = 3$ or 4. Thus, when the condition (55) is fulfilled, there is an over-screened Kondo effect with non Fermi liquid ground state. Note that this is not a necessary condition: When the inequality (55) is not satisfied, we cannot determine the nature of the ground state.

We now apply our analysis for elucidating the nature of the stable fixed points P_4 , P_5 and P_7 . For the fixed point P_4 , the ground state corresponds to the energy level with quantum number $\Sigma = 3$, and therefore there is an over-screened Kondo effect. Similarly, for the fixed point P_5 , the ground state corresponds to the energy level with quantum number $\Sigma = 4$, and therefore there is over-screened Kondo effect. Finally, for the fixed point P_7 , the ground state corresponds to the energy level with quantum number $\Sigma = 5$, and therefore we cannot conclude whether the impurity is over-screened or under-screened. As an example, when the initial values of the couplings λ_d , λ_q and λ_o are given by eq. (33), the Kondo Hamiltonian flows toward the fixed point P_5 , and therefore we conclude that there is an over-screened Kondo effect. In order to substantiate this statement, the exchange interaction between the ‘‘dressed’’ impurity atom and the Fermi sea should be considered. For this purpose, it is assumed that the temperature is low enough, so that the ‘‘dressed’’ impurity is in its ground state described by the wave functions (50), and the following representation of the identity operator is employed,

$$\begin{aligned} & \sum_{n,i,m} c_{n,i}^{\dagger} |\Sigma, m; g\rangle \langle \Sigma, m; g| c_{n,i} + \\ & + \sum_{n,i,m} c_{n,i} |\Sigma, m; g\rangle \langle \Sigma, m; g| c_{n,i}^{\dagger} = 1, \end{aligned}$$

where $|\Sigma, m; g\rangle$ describes the degenerate Fermi sea of the itinerate atoms and the ‘‘dressed’’ impurity. Then the exchange interaction of the ‘‘dressed’’ impurity with the itinerant atoms is

$$\begin{aligned} \tilde{H}_K = & \sum_{n,n'} \sum_{i,i'} \sum_{m,m'} \left\{ \langle \Sigma, m; g| c_{n',i'} H_K c_{n,i}^{\dagger} | \Sigma, m'; g\rangle - \right. \\ & \left. - \langle \Sigma, m; g| c_{n,i}^{\dagger} H_K c_{n',i'} | \Sigma, m'; g\rangle \right\} Y^{m,m'} c_{n',i'}^{\dagger} c_{n,i}, \end{aligned}$$

where $Y^{m,m'} = |\Sigma, m\rangle \langle \Sigma, m'|$ are Hubbard operators. Taking into account eqs. (5) and (50), we may write

$$\begin{aligned} \tilde{H}_K = & \frac{\tilde{\lambda}}{a_g^2} \sum_{n,n'} \sum_{i,i'} \sum_{m,m'} \sum_j \sum_{\{i\}_3} \sum_{\{i'\}_3} Y^{m,m'} c_{n',i'}^{\dagger} c_{n,i} \times \\ & \times C_{I,i_1;I,i_2;I,i_3;I,i;J,j}^{\Sigma,m} C_{I,i'_1;I,i'_2;I,i'_3;I,i';J,j}^{\Sigma,m'} \quad (56) \end{aligned}$$

where $C_{I,i_1;I,i_2;I,i_3;I,i;J,j}^{\Sigma,m}$ are the Clebsch-Gordan coefficients, $\{i\}_3 = \{i_1, i_2, i_3\}$ and $\{i'\}_3 = \{i'_1, i'_2, i'_3\}$. The coupling $\tilde{\lambda} \sim T_K$ is positive.

The Hamiltonian (56) is decomposed into a sum of multipole interactions, similar to the Hamiltonian (7). However, because of high spins that are involved [the dressed impurity has the spin $\Sigma = 4$ and the itinerant atoms have spin $I = \frac{5}{2}$], the exchange Hamiltonian consists of dipole, quadrupole, octupole, 16-pole and 32-pole interactions. Derivation of the scaling equations for this Hamiltonian is much more cumbersome than the derivation of the scaling equations for the bare Hamiltonian (7). Therefore we will be content with a qualitative picture pertaining to the Hamiltonian (56): The fact that $\tilde{\lambda} > 0$, implies that \tilde{H}_K displays an antiferromagnetic exchange interaction. This is a typical situation leading to over-screening Kondo effect, where the exchange interaction between the dressed impurity and the Fermi sea is anti-ferromagnetic^{4,8}. It can be shown that in the framework of second order poor man’s scaling technique, the anti-ferromagnetic coupling flows towards $\tilde{\lambda} \rightarrow \infty$, and therefore the weak coupling fixed point $\lambda \rightarrow \infty$ is unstable. Thus, the weak coupling fixed points $\lambda = 0$ and $\lambda \rightarrow \infty$ are unstable, implying that there is at least one stable strong coupling fixed point with finite λ ’s which describes a non Fermi phase⁸.

XI. ENTROPY, SPECIFIC HEAT AND MAGNETIC SUSCEPTIBILITY

We are now in a position to calculate a few experimentally relevant physical quantities. A possible candidate for elucidating the special features of the multipolar Kondo effect is the temperature dependence of numerous thermodynamic quantities. Here we compute the impurity contribution to the specific heat, the entropy, and the magnetic susceptibility, and compare some of our results with those obtained within the standard Kondo effect based on the $s - d$ Hamiltonian.

The formalism developed so far enables us to carry out these calculations in the weak coupling regime $T > T_K$, wherein it is expected that the general form of the thermodynamic quantities is dominated by logarithmic functions of $\frac{D}{T}$. Whereas for dipolar exchange interaction (governed by the $s - d$ Hamiltonian), the derivation is quite standard, the derivation and handling of the spin algebra in the present case of multipolar exchange interactions (carried out below) is more involved. It is found

that for the magnetic susceptibility, the temperature dependencies in the standard and multipolar Kondo effect are quite close to each other but for the specific heat and entropy the differences are quite sizeable. We are tempted to expect that in the strong coupling regime, the dependencies will be qualitatively and quantitatively distinct.

A. Entropy and Specific Heat

The impurity contributions to the entropy S_{imp} and the specific heat C_{imp} are given by,

$$S_{\text{imp}} = -k_B \frac{\partial(T \ln Z_{\text{imp}})}{\partial T}, \quad (57)$$

$$C_{\text{imp}} = T \frac{\partial S_{\text{imp}}}{\partial T}. \quad (58)$$

Here Z_{imp} is the partition function of the impurity⁴,

$$Z_{\text{imp}} = \frac{Z}{Z_c}, \quad (59)$$

where Z is the partition function of the total system and Z_c is the partition function of the itinerant atoms without impurity,

$$Z = \text{Tr}(e^{-\beta H}), \quad Z_c = \text{Tr}(e^{-\beta H_c}).$$

Perturbation calculations up to fourth order in the coupling constants yield the entropy (57),

$$S_{\text{imp}} = k_B \left\{ \ln(2F+1) + Z_3 + Z_4 \ln(\beta D) \right\}, \quad (60)$$

where

$$Z_3 = -\frac{2\pi^2}{3} \left\{ \frac{525}{2} \Lambda_d^3 - \frac{18213545952}{5} \Lambda_o^3 + 80640 \Lambda_q^2 \Lambda_d + 23514624 \Lambda_q^2 \Lambda_o + 39680928 \Lambda_o^2 \Lambda_d \right\}, \quad (61)$$

$$Z_4 = -\pi^2 \left\{ 525 \Lambda_d^4 + \frac{656474112}{5} \Lambda_q^4 + \frac{50025111034752}{25} \Lambda_o^4 + 1537536 \Lambda_d^2 \Lambda_q^2 + 1009659168 \Lambda_d^2 \Lambda_o^2 + 1065996288 \Lambda_d \Lambda_q^2 \Lambda_o - \frac{671877472896}{5} \Lambda_d \Lambda_o^3 - \frac{767799502848}{25} \Lambda_q^2 \Lambda_o^2 \right\}. \quad (62)$$

This result should be supported by the condition imposing the invariance of the entropy under the poor mans scaling transformation⁴, implying

$$\frac{\partial}{\partial \ln D} \left\{ Z_{\text{imp}}^{(3)}(\Lambda_d, \Lambda_q, \Lambda_o) + Z_4(\Lambda_d, \Lambda_q, \Lambda_o) \ln\left(\frac{D}{k_B T}\right) \right\} = 0. \quad (63)$$

Within the accuracy of this equation, when differentiating the second term, any implicit dependence on D through the couplings $\Lambda_{d,q,o}$ is neglected. The renormalization procedure should proceed until the bandwidth D is reduced to the temperature T . At this point, the fourth order perturbation theory contribution vanishes and the entropy takes the final form,

$$S_{\text{imp}} = k_B \left\{ \ln(2F+1) + Z_3(\Lambda_d(T), \Lambda_q(T), \Lambda_o(T)) \right\}, \quad (64)$$

where Z_3 (as a function of Λ_d , Λ_q and Λ_o) is given by eq. (61), whereas $\Lambda_{d,q,o}(T)$ are solution of the scaling equations (32).

The above results for the entropy pave the way for calculating the specific heat (58),

$$C_{\text{imp}} = k_B \frac{\partial}{\partial \ln T} \left[Z_3(\Lambda_d(T), \Lambda_q(T), \Lambda_o(T)) \right].$$

Taking into account the scaling equation (63), we get

$$C_{\text{imp}} = -k_B Z_4(\Lambda_d(T), \Lambda_q(T), \Lambda_o(T)), \quad (65)$$

where Z_4 (as a function of Λ_d , Λ_q and Λ_o) is given by eq. (62), whereas $\Lambda_{d,q,o}(T)$ are solution of the scaling equations (32).

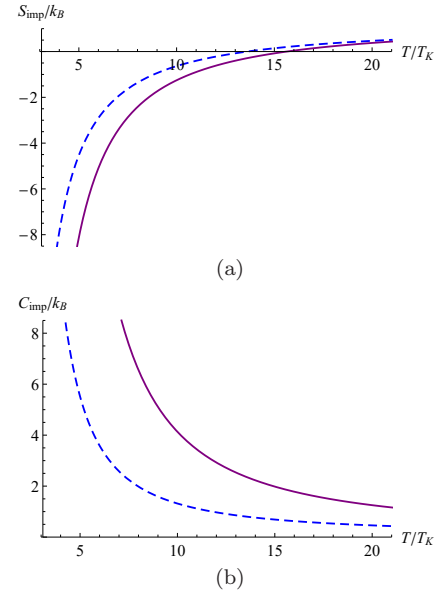


FIG. 10: (Color online) Results for $\lambda\rho_0 = 0.5$: Solid curves: The entropy (64) [panel (a)] and the specific heat (65) [panel (b)] for the $^{173}\text{Yb}(^1\text{S}_0) - ^{173}\text{Yb}(^3\text{P}_2)$ system governed by the multipolar Kondo Hamiltonian. Dashed curves: The entropy (66) [panel (a)] and the specific heat (67) [panel (b)] for the $^{171}\text{Yb}(^1\text{S}_0) - ^{171}\text{Yb}(^3\text{P}_2)$ system governed by the $s-d$ Kondo Hamiltonian.

The entropy (64) and the specific heat (65) of the impurity are shown in Fig. 10 for $\lambda\rho_0 = 0.5$ [solid curves in

panels (a) and (b)]. Fig. 10(a) illustrates decreasing of the entropy due to the Kondo interaction. The entropy of the isolated impurity atom is $\ln(2F + 1)$. Fig. 10(b) demonstrates a monotonic behaviour of the specific heat and the entropy in the weak coupling regime.

For comparison with the standard Kondo effect, consider the system consisting of $^{171}\text{Yb}(^1\text{S}_0)$ itinerant atoms and $^{171}\text{Yb}(^3\text{P}_2)$ localized impurities. In this case, the orbital angular momentum of the itinerant atoms is $I = \frac{1}{2}$, whereas the angular momentum of the localized impurity atoms is $F = \frac{3}{2}$ [the electronic orbital moment is $J = 2$, and the nuclear spin is $I = \frac{1}{2}$]. The entropy and the specific heat in this case are given by eqs. (3.4) and (3.5) in Ref.⁴. Taking into account the invariance of the entropy and the specific heat under the poor man's scaling, we get the following expressions,

$$S_{s-d} = k_B \left\{ \ln(2F + 1) - \frac{\pi^2}{3} F(F + 1) \Lambda_{s-d}^3(T) \right\}, \quad (66)$$

$$C_{s-d} = k_B \pi^2 F(F + 1) \Lambda_{s-d}^4(T), \quad (67)$$

where

$$\Lambda_{s-d}(T) = \frac{1}{\ln(T/T_K)}. \quad (68)$$

The entropy (66) and the specific heat (67) for the $^{171}\text{Yb}(^1\text{S}_0) - ^{171}\text{Yb}(^3\text{P}_2)$ system is shown in Fig. 10 [dashed curves in panels (a) and (b)].

B. Magnetic Susceptibility

In order to derive an expression for the magnetic susceptibility of the atomic gas with the Kondo impurity, we note that the itinerant atoms are in the electronic spin-singlet state, whereas the impurity is in the electronic spin-triplet state. Therefore interaction of itinerant atoms with the magnetic field is proportional to the nuclear magneton μ_n , whereas the interaction of the impurity with the magnetic field is proportional to the Bohr magneton μ_B . The interaction of the itinerant atoms and the impurity with the magnetic field $\mathbf{B} = B\mathbf{e}_z$ is described by the Hamiltonian,

$$H_B = -g_{\text{Yb}}\mu_n \sum_{i,i',n} (\mathbf{B} \cdot \mathbf{I}_{i,i'}) c_{n,i}^\dagger c_{n,i'} - g\mu_B \sum_f (\mathbf{B} \cdot \mathbf{F}_{f,f'}) X^{f,f'}, \quad (69)$$

where $g_{\text{Yb}} = -0.2592$ is the nuclear g-factor of ^{173}Yb ³⁸, g is electronic g-factor of Yb atom in the $^3\text{P}_2$ state,

$$g = \frac{3J(J + 1) + S(S + 1) - \ell(\ell + 1)}{2J(J + 1)} = \frac{3}{2}, \quad (70)$$

where for the $^3\text{P}_2$ configuration, $J = 2$ and $\ell = S = 1$ [in this section, S and ℓ denote the electronic spin and

orbital angular momentum of the $\text{Yb}(^3\text{P}_2)$ atom]. Then the impurity magnetization $\mathbf{M}_{\text{imp}} = M_{\text{imp}}\mathbf{e}_z$ can be written as⁴,

$$M_{\text{imp}} = g\mu_B \langle \hat{F}^z \rangle + g_{\text{Yb}}\mu_n \left\{ \langle \hat{I}^z \rangle - \langle \hat{I}^z \rangle_0 \right\}, \quad (71)$$

where $\langle \dots \rangle$ indicates a thermal average with respect to the total Hamiltonian $H + H_B$, and $\langle \dots \rangle_0$ with respect to $H_0 + H_B$,

$$\langle \mathcal{O} \rangle = \frac{\text{tr}(e^{-\beta(H+H_B)} \mathcal{O})}{\text{tr} e^{-\beta(H+H_B)}},$$

$$\langle \mathcal{O} \rangle_0 = \frac{\text{tr}(e^{-\beta(H_0+H_B)} \mathcal{O})}{\text{tr} e^{-\beta(H_0+H_B)}}.$$

Here H and H_0 are given by eq. (2).

The magnetic interaction described by the Hamiltonian (69) has a standard form of a scalar product of the external magnetic field and the magnetic dipole angular momentum operators of the impurity and itinerant atoms. It reflects the fact that (usually), only the dipole moment contributes to the linear magnetization of atoms. However, somewhat unexpectedly, the Kondo Hamiltonian (7) gives rise to nontrivial contributions of the quadrupole and octupole magnetic moments to the linear magnetization of the system. This requires an analysis that is distinct from the one employed in the standard treatment of magnetic susceptibility as applied to the $s - d$ Hamiltonian. Here we derive the magnetic susceptibility of the multipolar Kondo Hamiltonian (as a function of temperature), in the weak coupling regime, $T \gg T_K$.

C. Contributions to M_{imp} due to H_K

First, let us recall the expression for the magnetization of an isolated atom. To linear order in the magnetic field B , the magnetization of a single ^{173}Yb atom in the $^3\text{P}_2$ state with $F = \frac{3}{2}$ is,

$$M_{\text{imp}}^{(0)} = \frac{F(F + 1)}{3T} (g\mu_B)^2 B. \quad (72)$$

Next, consider the contributions to M_{imp} due to H_K ,

$$\delta M_{\text{imp}} = M_{\text{imp}} - M_{\text{imp}}^{(0)}.$$

By definition, this contribution is given by,

$$\delta M_{\text{imp}} = g\mu_B \left\{ \langle \hat{F}^z \rangle - \langle \hat{F}^z \rangle_0 \right\} + g_{\text{Yb}}\mu_n \left\{ \langle \hat{I}^z \rangle - \langle \hat{I}^z \rangle_0 \right\}. \quad (73)$$

Assuming that the couplings λ 's are small and expanding δM_{imp} with powers of H_K yield,

$$\delta M_{\text{imp}} = \sum_{n=1}^{\infty} \delta M_{\text{imp}}^{(n)}, \quad (74)$$

where $\delta M_{\text{imp}}^{(n)}$ is proportional to λ_β^n . Below we will calculate $\delta M_{\text{imp}}^{(1)}$ and $\delta M_{\text{imp}}^{(2)}$.

1. Corrections linear with λ 's

The correction $\delta M_{\text{imp}}^{(1)}$ can be written as,

$$\delta M_{\text{imp}}^{(1)} = \sum_{\beta} \left\{ \delta M_{f;\beta} + \delta M_{i;\beta} \right\}. \quad (75)$$

Here

$$\delta M_{f;\beta} = -g\mu_B \int_0^{\beta} \left\langle \hat{F}^z H_{\beta}(\tau) \right\rangle_0 d\tau, \quad (76)$$

$$\delta M_{i;\beta} = -g_{Yb}\mu_n \int_0^{\beta} \left\langle \hat{I}^z H_{\beta}(\tau) \right\rangle_0 d\tau. \quad (77)$$

The expectation values $\langle F^{\alpha\beta} \rangle$, $\langle I^{\alpha\beta} \rangle$, $\langle F^z F^{\alpha\beta} \rangle$ and $\langle I^z I^{\alpha\beta} \rangle$ [where $\hat{F}^{\alpha\beta}$ or $\hat{I}^{\alpha\beta}$ are dipole ($\beta = d$), quadrupole ($\beta = q$) and octupole ($\beta = o$) tensors for a localized impurity or itinerant atoms, α 's are the Cartesian indices] are calculated in Appendix I. Then $\delta M_{\text{imp}}^{(1)}$ takes the form,

$$\delta M_{\text{imp}}^{(1)} = -\frac{175B}{4T} g\mu_B g_{Yb}\mu_n \Lambda_d. \quad (78)$$

Note that the factor $\frac{175}{4}$ comes from,

$$\frac{2}{9} F(F+1) I(I+1)(2I+1) = \frac{175}{4}.$$

If instead of itinerant atoms with spin $I = \frac{5}{2}$, we use atoms with spin $s = \frac{1}{2}$, the last expression turns out to be,

$$\frac{2}{9} F(F+1) s(s+1)(2s+1) = \frac{F(F+1)}{3},$$

which agrees with eq. (3.2) from Ref.⁴.

2. Corrections quadratic with λ 's

Calculating the second order correction, $\delta M_{\text{imp}}^{(2)}$, we get δM_{imp} up to λ^2 ,

$$\begin{aligned} \delta M_{\text{imp}} &= -M_{\text{imp}}^{(0)} N(I) \frac{g\mu_B}{g_{Yb}\mu_n} \times \\ &\times \left\{ \Lambda_d - \mathfrak{F}_d^{(2)} \ln \left(\frac{D}{T} \right) \right\}, \end{aligned} \quad (79)$$

where $M_{\text{imp}}^{(0)}$ is given by eq. (72), $N(I)$ is given by eq. (1), and

$$\begin{aligned} \mathcal{N}_I &= \frac{2}{3} I(I+1)(2I+1), \quad (80) \\ \mathfrak{F}_d^{(2)} &= -\Lambda_d^2 - \frac{9216}{25} \Lambda_q^2 - \frac{1469664}{25} \Lambda_o^2. \end{aligned} \quad (81)$$

$\mathfrak{F}_d^{(2)}$ is obtained from eq. (44a) neglecting the terms of order λ^3 . The condition imposing the invariance of the magnetization under the poor man scaling transformation is

$$\frac{\partial}{\partial \ln D} \left\{ \Lambda_d - \mathfrak{F}_d^{(2)} \ln \left(\frac{D}{T} \right) \right\} = 0. \quad (82)$$

Within the accuracy of this equation, when differentiating the second term, we should neglect any implicit dependence on D through the couplings Λ_{β} . The renormalization procedure should proceed until the bandwidth D is reduced to the temperature T . At this point, the second order of the perturbation theory vanishes and the magnetization takes the form,

$$M_{\text{imp}} = M_{\text{imp}}^{(0)} \left\{ 1 - \frac{g_{Yb}\mu_n}{g\mu_B} N(I) \Lambda_d(T) \right\}, \quad (83)$$

where $N(I)$ is given by eq. (1), $\Lambda_d(T)$ is the solution of the second order scaling equation (32).

It is useful to write the magnetic susceptibility $\chi_{\text{imp}} = \partial M_{\text{imp}} / \partial B$ as,

$$\chi_{\text{imp}}(T) = \chi_{\text{imp}}^{(0)} + \delta\chi_{\text{imp}}(T), \quad (84)$$

where $\chi_{\text{imp}}^{(0)}$ is the susceptibility of the isolated impurity atom, and $\delta\chi_{\text{imp}}(T)$ is correction to the susceptibility due to the Kondo interaction. Explicitly,

$$\chi_{\text{imp}}^{(0)} = \frac{\chi_0}{3} \frac{T_K}{T} F(F+1), \quad (85)$$

$$\delta\chi_{\text{imp}} = X_{\text{imp}} N(I) \Lambda_d, \quad (86)$$

where

$$\chi_0 = \frac{(g\mu_B)^2}{T_K}, \quad X_{\text{imp}} = -\frac{g_{Yb}\mu_n}{g\mu_B} \chi_{\text{imp}}^{(0)}.$$

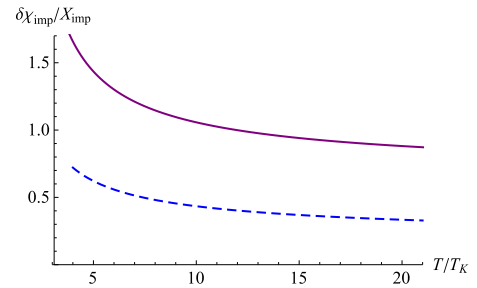


FIG. 11: (Color online) Solid curve: The ratio $\delta\chi_{\text{imp}}/\chi_{\text{imp}}$ (86) as a function of T for $\lambda a_g^2 \rho_0 = 0.5$. The values of the parameters are $\Lambda_d^{(0)} = 0.0247619$, $\Lambda_q^{(0)} = -0.0005952$, $\Lambda_o^{(0)} = -0.0002646$. Dashed curve: The ratio $\delta\chi_{s-d}/\chi_{\text{imp}}$ (87) for the $^{171}\text{Yb}(^1\text{S}_0) - ^{171}\text{Yb}(^3\text{P}_2)$ system.

The ratio $\delta\chi_{\text{imp}}/\chi_{\text{imp}}$ as a function of temperature is shown in Fig. 11, solid curve. It should be noted that $X_{\text{imp}}/\chi_{\text{imp}}^{(0)} \ll 1$ since the ratio,

$$\frac{g_{Yb} \mu_n}{g \mu_B} = -9.411 \cdot 10^{-5},$$

is small. When T approaches the Kondo temperature, $\delta\chi_{\text{imp}}$ diverges as $1/\ln(T/T_K)$ which indicates breaking down of the underlying perturbation theory.

For comparison, consider a system consisting of $^{171}\text{Yb}(^1\text{S}_0)$ itinerant atoms and a $^{171}\text{Yb}(^3\text{P}_2)$ atom as localized impurity. The atomic orbital angular momentum is assumed to be $F = \frac{3}{2}$, therefore the susceptibility of the isolated impurity is given by eq. (85). Magnetic susceptibility of the $^{171}\text{Yb}(^3\text{P}_2)$ atom interacting with the $^{171}\text{Yb}(^1\text{S}_0)$ atoms [atomic orbital moment is $I = \frac{1}{2}$] is⁴,

$$\begin{aligned}\chi_{s-d} &= \chi_{\text{imp}}^{(0)} + \delta\chi_{s-d}, \\ \delta\chi_{s-d} &= X_{\text{imp}} \Lambda_{s-d}(T),\end{aligned}\quad (87)$$

where $\Lambda_{s-d}(T)$ is given by eq. (68). The ratio $\delta\chi_{s-d}/X_{\text{imp}}$, eq. (87), is shown in Fig. 11, dashed curve.

D. Experimental Feasibility

Having developed the theoretical framework for calculating entropy, specific heat and magnetization, a few words on the experimental feasibility of measuring thermodynamic quantities (specific for the pertinent system), are in order. It is worth mentioning that some of these thermodynamic observables have been successfully measured in one-component Bose gases⁴³, two-component Fermi gases⁴⁴, and $\text{SU}(N)$ fermions trapped in optical lattices⁴⁵ either using *in-situ* local probe of the inhomogeneous atomic density^{44,46} or performing a spin transport measurements⁴⁷. In particular, the magnetic susceptibility of the two-component Fermi gas is determined in various ways, including (1) the relative spin fluctuation measurement⁴⁸, (2) the sum-rule approach for the spin-dipole mode frequency⁴⁷ or (3) the direct measurement of susceptibility from the inhomogeneous density profile of the spin-imbalanced atomic gas⁴⁹. Similar measurements should be feasible in a $^1\text{S}_0$ - $^3\text{P}_2$ ytterbium mixture. Indeed, the spin-dependent trapping potential available in the ytterbium mixture allows one to induce spin-selective transport and consequently monitor the spin-dipole mode of the system. In a similar manner, the heat capacity of the two-component gas can be determined from the local density of the atomic gas⁵⁰.

XII. CONCLUSION

Let us then briefly summarize our results. Our main arena concerns the Kondo physics in an ultracold Fermi gas of $^{173}\text{Yb}(^1\text{S}_0)$ atoms (in their electronic ground-state) in which a few $^{173}\text{Yb}(^3\text{P}_2)$ atoms (in a long lived excited state) are trapped in a specially designed optical potential. The main objectives are: 1) To explore the feasibility of experimental realization; 2) To calculate the exchange interaction between the itinerant $^{173}\text{Yb}(^1\text{S}_0)$ and $^{173}\text{Yb}(^3\text{P}_2)$ atoms and to verify that it is an antiferromagnetic exchange; 3) To construct the Kondo Hamiltonian

and to identify its underlying symmetry; 4) To carry out the corresponding poor-man scaling, to identify the stable fixed points and to determine whether some of them display non-Fermi liquid behaviour; 5) To calculate some experimentally accessible observable in such a system.

As far as objective 1) is concerned, we have considered a mixture of $^1\text{S}_0$ and $^3\text{P}_2$ ytterbium fermions that can be readily prepared in contemporary experiments, in which a state-dependent optical potential employs a strong $^3\text{P}_2$ - $^3\text{S}_1$ transition and tightly confines $^3\text{P}_2$ atoms while leaves the ground-state $^1\text{S}_0$ atoms itinerant. By properly choosing the wavelength of the optical potential, we have shown that the spontaneous light scattering can be sufficiently reduced to observe a many-body effect. The localized and itinerant atoms can be independently detected with the combination of an optical pumping and a blast. Finally a $^1\text{S}_0$ - $^3\text{P}_2$ mixture of ytterbium atoms displays a magnetic Feshbach resonance by which the interaction strength between localized and itinerant atoms can be further controlled⁴². Such novel features may open a new route to investigate the Kondo effect with tuneable atom-atom interactions in this system. Calculating the exchange interaction proceeds along similar lines as in our previous paper³³.

The main difficulty is encountered in achieving goals (3) and (4). It is required to write down the Kondo Hamiltonian in terms of multipole expansion, since otherwise, the RG procedure is inapplicable. This requires a technically tedious procedure related to the pertinent spin algebra. Moreover, identifying the corresponding fixed points requires calculations of RG diagrams to third order in the exchange constant, which turn out to be rather involved. Details of the calculations are explained in the Appendices.

Having overcome these technical difficulties, we have found seven fixed points for λ_d and λ_q and λ_o . Three of them, P_4 , P_5 and P_7 [eqs. (45d), (45e) and (45g)] are stable, and the other fixed points are unstable. The fixed points found here are distinct from the NB non Fermi liquid fixed point described in our previous paper¹³, in which we studied the Kondo physics in a mixture of ^{23}Na and ^6Li atoms. In the present work, the NB non Fermi liquid fixed point corresponds to P_1 in the list (45d), that is found to be *unstable*.

The remaining task, that is, elucidating the Kondo physics *in the strong coupling regime* for the new stable fixed points P_4 , P_5 and P_7 (identified in this work) is beyond the scope of our present study. It is perceived that the standard techniques that are applied to the dipolar Kondo effect such as Bethe Ansatz and conformal field theory might work also in this case albeit with non-trivial modifications.

Acknowledgement

Y.A, I.K and T.K acknowledge many years of collaboration and discussions pertaining to the Kondo Physics with their colleague and their close friend

Konstantin Abramovich Kikoin.

His sudden death left us shocked and wordless.

The authors thank S. Zhang for useful discussion. G.B.J acknowledges financial support from the Hong Kong Research Grants Council (Project No. 26300014/16300215/16311516) and from the Croucher Foundation. The research of Y.A is partially supported by grant 400/12 of the Israel Science Foundation.

Appendix A: Trapping of the Yb Atoms by the Optical Potential

Since the Yb(3P_2) atom has the electronic orbital moment $J = 2$, the polarizability $\hat{\alpha}_e(\omega)$ is a 5×5 matrix. We introduce the matrices $\hat{\alpha}_e^x(\omega)$, $\hat{\alpha}_e^y(\omega)$ and $\hat{\alpha}_e^z(\omega)$, for the electric field collinear to the axes x , y and z , respectively. Explicitly, they are

$$\begin{aligned}\hat{\alpha}_e^z &= \text{diag}(\alpha_2, \alpha_1, \alpha_0, \alpha_1, \alpha_2), \\ \hat{\alpha}_e^\beta &= \hat{U}_\beta \hat{\alpha}_e^z \hat{U}_\beta^\dagger,\end{aligned}\quad (\text{A1})$$

where $\beta = x, y$ is a Cartesian index, the spin-rotation matrices \hat{U}_β are

$$\hat{U}_x = e^{i\pi \hat{J}^x / 2}, \quad \hat{U}_y = e^{-i\pi \hat{J}^y / 2}.$$

We consider the optical potential generated by standing electromagnetic wave in the directions of the axes x, y and z with the double-magic wavelength λ_0 ³²,

$$\lambda_0 = 546 \text{ nm}. \quad (\text{A2})$$

The polarizability $\hat{\alpha}_F^\beta(\lambda_0) = \alpha_e(\lambda_0) \hat{J}^0$ [the Cartesian index β indicates the direction of the electric field] is proportional to the identity matrix \hat{J}^0 . Explicitly, $\alpha_g(\lambda_0)$ and $\alpha_e(\lambda_0)$, the polarizability of the Yb(1S_0) and Yb(3P_2) atoms are³²

$$\alpha_e(\lambda_0) = 250 \text{ a.u.}, \quad \alpha_g(\lambda_0) = 200 \text{ a.u.} \quad (\text{A3})$$

1. Optical Potential

We consider possibility of formation of the short- and long-wavelength potentials the light of the double-magic wavelength λ_0 . The optical potential is generated by three pairs of lasers, as illustrated in Fig. 12. The light of the first, second or third pair of lasers propagates parallel and antiparallel to the axes x , y or z . The optical potential is,

$$V_\nu(\mathbf{r}) = -\alpha_\nu(\omega) \lim_{\mathcal{T} \rightarrow \infty} \frac{1}{\mathcal{T}} \int_0^{\mathcal{T}} |\mathbf{E}(\mathbf{r}, t)|^2 dt, \quad (\text{A4})$$

where $\nu = g$ or e for the Yb(1S_0) or Yb(3P_2) atoms. The electric field $\mathbf{E}(\mathbf{r})$ is,

$$\mathbf{E}(\mathbf{r}, t) = \sum_{\beta=1}^6 \mathbf{E}_\beta(\mathbf{r}, t). \quad (\text{A5})$$

Here

$$\begin{aligned}\mathbf{E}_\beta(\mathbf{r}, t) &= \mathbf{E}_\beta^{(0)} \cos(\mathbf{k}_\beta \mathbf{r} - \omega_0 t) \times \\ &\times \exp\left(-\frac{x_{a_\beta}^2 - x_{b_\beta}^2}{2L^2}\right),\end{aligned}\quad (\text{A6})$$

where $\mathbf{E}_\beta^{(0)} = E_u \mathbf{e}_{a_\beta}$, $\mathbf{E}_{\beta+3}^{(0)} = E_v \mathbf{e}_{a_\beta}$, $\beta = 1, 2, 3$. The indices $a_\beta = a_{\beta+3}$ and $b_\beta = b_{\beta+3}$ are

$$\begin{aligned}a_1 &= 2, & a_2 &= 3, & a_3 &= 1, \\ b_1 &= 3, & b_2 &= 1, & b_3 &= 2.\end{aligned}\quad (\text{A7})$$

\mathbf{e}_1 , \mathbf{e}_2 and \mathbf{e}_3 are unit vectors parallel to the axes x , y and z . The amplitudes E_u and E_v are real and satisfy the inequalities

$$E_u \gg E_v > 0.$$

The wave vectors of the light are $\mathbf{k}_\beta = -\mathbf{k}_{\beta+3} = k_0 \mathbf{e}_\beta$, where $\beta = 1, 2, 3$, $k_0 = 2\pi_0/\lambda_0$ is the wavenumber of the light. $\omega_0 = k_0 c$ is the frequency of the light. The waist radius $\sqrt{2}L$ satisfies the inequality

$$k_0 L \gg 1.$$

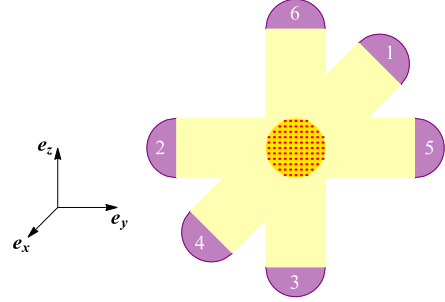


FIG. 12: (Color online) Three pairs of lasers labelled by the numbers 1 – 6 generating trapping optical potential [golden yellow disk with red dots].

Explicitly, the optical potential is

$$V_\nu(\mathbf{r}) = V_\nu^{(\text{slow})}(\mathbf{r}) + V_\nu^{(\text{fast})}(\mathbf{r}). \quad (\text{A8})$$

Here

$$V_\nu^{(\text{slow})}(\mathbf{r}) = \sum_{\beta=1}^3 V_{\beta,\nu}^{(\text{slow})}(\mathbf{r}), \quad (\text{A9})$$

$$V_\nu^{(\text{fast})}(\mathbf{r}) = \sum_{\beta=1}^3 V_{\beta,\nu}^{(\text{fast})}(\mathbf{r}), \quad (\text{A10})$$

where

$$V_{\beta,\nu}^{(\text{slow})}(\mathbf{r}) = -V_{0,\nu} \exp\left(-\frac{x_{a_\beta}^2 + x_{b_\beta}^2}{L^2}\right), \quad (\text{A11})$$

$$\begin{aligned}V_{\beta,\nu}^{(\text{fast})}(\mathbf{r}) &= -V_{1,\nu} \cos(2k_0 x_\beta) \times \\ &\times \exp\left(-\frac{x_{a_\beta}^2 + x_{b_\beta}^2}{L^2}\right).\end{aligned}\quad (\text{A12})$$

The strengths $V_{0,\nu}$ and $V_{1,\nu}$ are

$$\begin{aligned} V_{0,\nu} &= \frac{\alpha_\nu(\omega_0)}{2} \{E_u^2 + E_v^2\}, \\ V_{1,\nu} &= \alpha_\nu(\omega_0) E_u E_v. \end{aligned} \quad (\text{A13})$$

We assume that E_u and E_v are real and positive and $\alpha_\nu(\lambda_0) > 0$, and therefore $V_{0,\nu} > 0$ and $V_{1,\nu} > 0$. Here β is a Cartesian index, the indices a_β and b_β are given by eq. (A7).

The optical potential (A8) is illustrated in Fig. 2 for $L = 10\lambda_0$ and $E_v = 0.05E_u$. Here the solid blue and green curves show $V_\nu(x, 0, 0)$ and $V_\nu(x, \lambda_0/4, \lambda_0/4)$. For comparison, the dashed red curve illustrates $V_\nu^{(\text{slow})}(x, 0, 0)$, eq. (A9). Note that we take here $L = 10\lambda_0$ just for better illustration. Real values of L are larger than $10^2\lambda_0$.

In the following discussions, we assume that the $\text{Yb}(^3\text{P}_2)$ atoms are trapped by the fast oscillating potential (A10) and are localized near the stable equilibrium points $\mathbf{r} = (n_1\lambda_0/2, n_2\lambda_0/2, n_3\lambda_0/2)$, where n_1, n_2 and n_3 are integers. From the other side, we assume that the density of the $\text{Yb}(^1\text{S}_0)$ atoms is such that the Fermi energy ϵ_F [measured from the bottom of the potential well] satisfies the inequality $\epsilon_F \gg V_{1,g}$, and therefore the atoms with energy close to ϵ_F can be considered as itinerant: their motion is restricted by the potential $V_g^{(\text{slow})}(\mathbf{r})$, eq. (A9).

2. Wave Function and Energy of the Trapped $\text{Yb}(^3\text{P}_2)$ Atoms

The density of the $\text{Yb}(^3\text{P}_2)$ atoms are low, so that all the atoms are localized by the fast oscillating potential (A10). When the energy level of the atom is deep enough, we can derive the wave function and the energy level in harmonic approximation. Consider, for example, the atom trapped near the stable equilibrium point $\mathbf{r} = (0, 0, 0)$. When the radius of localization of the atom is small with respect to $\lambda_0/4$, the optical potential (A10) can be approximated as,

$$V_e^{(\text{fast})}(\mathbf{r}) \approx -V_{1,e} + 2V_{1,e} (k_0 r)^2, \quad (\text{A14})$$

whereas $V_e^{(\text{slow})}(\mathbf{r})$ is almost constant for $r < \lambda_0/4$, where $r = |\mathbf{r}|$. The wave function of the atom trapped by the harmonic potential (A14) is given by eq. (15).

The energy ϵ_{imp} measured from the bottom of the well is,

$$\epsilon_{\text{imp}} = \frac{3}{2} \hbar\Omega_e. \quad (\text{A15})$$

3. Wave Functions and Energy Levels of the Trapped $\text{Yb}(^1\text{S}_0)$ Atoms

When the energy ϵ of the trapped $\text{Yb}(^1\text{S}_0)$ atom [measured from the bottom of the potential well] satisfies the

inequality $\epsilon \gg V_{1,g}$, we can approximate the potential (A8) as

$$V_g(\mathbf{r}) \approx V_g^{(\text{slow})}(\mathbf{r}). \quad (\text{A16})$$

Moreover, when the energy level is deep enough, we can approximate $V_g^{(\text{slow})}(\mathbf{r})$ as,

$$V_g^{(\text{slow})}(\mathbf{r}) \approx -3V_{0,g} + 2V_{0,g} \frac{r^2}{L^2}. \quad (\text{A17})$$

Quantum states of atoms in isotropic potential are described by the radial quantum number n [$n = 0, 1, 2, \dots$], the angular momentum l [$l = 0, 1, 2, \dots$] and projection m of the angular momentum on the axis z [$m = -l, -l + 1, \dots, l$]. Due to the centrifugal barrier, only the atoms with $l = 0$ can approach the impurity and be involved in the exchange interaction with it. The wave functions of the atoms with $l = 0$ trapped by the harmonic potential (A17) are,

$$\Psi_n(\mathbf{r}) = \frac{\mathcal{N}_n}{\sqrt{4\pi}} L_n^{(\frac{1}{2})} \left(\frac{r^2}{a_g^2} \right) \exp \left(-\frac{r^2}{2a_g^2} \right), \quad (\text{A18})$$

where $L_n^{(\frac{1}{2})}(\varrho)$ are generalized Laguerre polynomials. The normalization factor is

$$\mathcal{N}_n = \left(\frac{2}{\pi a_g^6} \right)^{1/4} \sqrt{\frac{2^{n+2} n!}{(2n+1)!}}.$$

The harmonic length a_g and frequency Ω_g are defined as

$$\frac{a_g}{L} = \left(\frac{\mathcal{E}_L}{2V_{0,g}} \right)^{1/4}, \quad \hbar\Omega_g = 2\sqrt{2\mathcal{E}_L V_{0,g}}, \quad (\text{A19})$$

where \mathcal{E}_L is defined as,

$$\mathcal{E}_L = \frac{\hbar^2}{2ML^2}. \quad (\text{A20})$$

The energy levels of the states with $l = 0$ are,

$$\epsilon_n = \hbar\Omega_g \left(2n + \frac{3}{2} \right). \quad (\text{A21})$$

In what following we assume that

$$\Omega_e \gg \Omega_g. \quad (\text{A22})$$

Within this framework, the spectrum is nearly continuous and the ytterbium atoms in the ground-state form a Fermi gas. The Fermi energy ϵ_F is such that $\epsilon_F \gg \hbar\Omega_g$, hence the Fermi gas is 3D.

Appendix B: Multipole Operators

In subsections B1 and B2 we introduced multipole operators: A 2^n pole operator is an expression involving n spin operators, with appropriate coefficients. These operators, explicitly calculated in this section, are the building blocks of the exchange interaction of the multipolar Kondo Hamiltonian to be introduced in the next section.

1. Notations

In this subsection we introduce the definitions and expressions for the 2^n poles required for the representation of the Kondo Hamiltonian in terms of multipole expansion. These 2^n poles result from the spin content of the underlying atomic system.

We consider exchange interaction of itinerant atoms (which are ^{173}Yb atoms in the ground $^1\text{S}_0$ state with atomic spin $I = \frac{5}{2}$), and localized impurities (which are the same ^{173}Yb atoms in the long lived excited $^3\text{P}_2$ state with atomic spin $F = \frac{3}{2}$). Note that I is contributed solely from the nuclear spin while F is the sum of electronic and nuclear spins. An atom with total angular momentum $F = \frac{3}{2}$ has nontrivial dipole, quadrupole and octupole magnetic momenta. They are denoted here as

$$\hat{F}^\alpha, \quad \hat{F}^{\alpha,\alpha'}, \quad \hat{F}^{\alpha,\alpha',\alpha''},$$

where α, α' and α'' are Cartesian indices. An atom with total angular momentum $I = \frac{5}{2}$ has nontrivial dipole, quadrupole, octupole, 16-pole and 32-pole magnetic momenta, denoted here as

$$\begin{aligned} \hat{I}^{\alpha_1}, \quad \hat{I}^{\alpha_1,\alpha_2}, \quad \hat{I}^{\alpha_1,\alpha_2,\alpha_3}, \\ \hat{I}^{\alpha_1,\alpha_2,\alpha_3,\alpha_4}, \quad \hat{I}^{\alpha_1,\alpha_2,\alpha_3,\alpha_4,\alpha_5}. \end{aligned}$$

When an expression applies for both itinerant atoms and impurities, we use the notations $\hat{S}^\alpha, \hat{S}^{\alpha,\alpha'}, \hat{S}^{\alpha,\alpha',\alpha''}$ for the dipole, quadrupole and octupole angular momenta. Here \hat{S} denotes the operators \hat{F} or \hat{I} .

2. Explicit expressions for 2^n -Pole Momenta

The magnetic dipole operator is collinear with the vector of its spin (more precisely its total angular momentum) operator. When a particle has spin S , the vector \mathbf{S} of the spin matrices (generators of the $2S+1$ -dimensional representation of the $\text{SU}(2)$ group) are,

$$\begin{aligned} S_{s,s'}^z &= s \delta_{s,s'}, \\ S_{s,s'}^+ &= \mathcal{L}(S, s) \delta_{s,s'+1}, \\ S_{s,s'}^- &= \mathcal{L}(S, s') \delta_{s',s+1}, \end{aligned} \quad (\text{B1})$$

where s, s' are magnetic quantum numbers such that $|s| \leq S$, and

$$\mathcal{L}(S, s) = \sqrt{(S+s)(S-s+1)}.$$

Next, the quadrupole moment operators are represented by symmetric traceless matrices $S^{\alpha,\alpha'}$ ($\alpha, \alpha' = x, y, z$ are Cartesian indices) defined as,

$$\hat{S}^{\alpha,\alpha'} = \left\{ \hat{S}^\alpha, \hat{S}^{\alpha'} \right\} - \frac{2}{3} \hat{\mathbf{S}}^2 \delta^{\alpha,\alpha'}, \quad (\text{B2})$$

where

$$\left\{ \hat{S}^\alpha, \hat{S}^{\alpha'} \right\} = \hat{S}^\alpha \hat{S}^{\alpha'} + \hat{S}^{\alpha'} \hat{S}^\alpha.$$

The quadrupole operators satisfy the following equalities,

$$\hat{S}^{\alpha,\alpha'} = \hat{S}^{\alpha',\alpha}, \quad \sum_{\alpha} \hat{S}^{\alpha,\alpha} = 0. \quad (\text{B3})$$

Continuing this analysis, the octupole moment operators are represented by matrices,

$$\begin{aligned} \hat{S}^{\alpha,\alpha',\alpha''} &= \left\{ \hat{S}^\alpha, \hat{S}^{\alpha'}, \hat{S}^{\alpha''} \right\} - \frac{1}{5} \left(3 \hat{\mathbf{S}}^2 - 1 \right) \times \\ &\times \sum_{\alpha_1, \alpha'_1, \alpha''_1} P_{\alpha_1, \alpha'_1, \alpha''_1}^{\alpha, \alpha', \alpha''} \delta^{\alpha_1, \alpha'_1} \hat{S}^{\alpha''_1}. \end{aligned} \quad (\text{B4})$$

Here the symbol $P_{\alpha_1, \alpha'_1, \alpha''_1}^{\alpha, \alpha', \alpha''}$ denotes permutation of the indices $\alpha, \alpha', \alpha''$,

$$\begin{aligned} P_{\alpha_1, \alpha'_1, \alpha''_1}^{\alpha, \alpha', \alpha''} &= \delta_{\alpha, \alpha_1} P_{\alpha'_1, \alpha''_1}^{\alpha', \alpha''} + \delta_{\alpha, \alpha'_1} P_{\alpha''_1, \alpha_1}^{\alpha', \alpha''} + \\ &+ \delta_{\alpha, \alpha''_1} P_{\alpha_1, \alpha'_1}^{\alpha', \alpha''}, \end{aligned} \quad (\text{B5})$$

the symbol $P_{\alpha_1, \alpha'_1}^{\alpha, \alpha'}$ denotes permutation of the indices α, α' ,

$$P_{\alpha_1, \alpha'_1}^{\alpha, \alpha'} = \delta_{\alpha, \alpha_1} \delta_{\alpha', \alpha'_1} + \delta_{\alpha, \alpha'_1} \delta_{\alpha', \alpha_1}. \quad (\text{B6})$$

The symbol $\left\{ \hat{S}^\alpha, \hat{S}^{\alpha'}, \hat{S}^{\alpha''} \right\}$ is fully symmetric product of $\hat{S}^\alpha, \hat{S}^{\alpha'}$ and $\hat{S}^{\alpha''}$,

$$\left\{ \hat{S}^{\alpha_1}, \hat{S}^{\alpha_2}, \hat{S}^{\alpha_3} \right\} = \sum_{\{\alpha'\}_3} P_{\alpha'_1, \alpha'_2, \alpha'_3}^{\alpha_1, \alpha_2, \alpha_3} \hat{S}^{\alpha'_1} \hat{S}^{\alpha'_2} \hat{S}^{\alpha'_3},$$

where $\{\alpha'\}_3 = \{\alpha'_1, \alpha'_2, \alpha'_3\}$. The octupole operators are symmetric with all the indices,

$$\hat{S}^{\alpha,\alpha',\alpha''} = \hat{S}^{\alpha',\alpha,\alpha''} = \hat{S}^{\alpha,\alpha'',\alpha'}.$$

Moreover, they are constructed in such a way that the trace over any two indices vanishes that is,

$$\sum_{\alpha'} \hat{S}^{\alpha,\alpha',\alpha'} = 0.$$

Appendix C: Exchange Interaction

Appendices C, D, E, F main points: The second order correction terms are defined in Eqs. (30, 31), while the third ordered correction terms are defined in Eqs. (39). The formidable task of evaluating these terms is carried out in these subsections.

When an impurity atom is localized at the origin of coordinates and an itinerant atom is placed at position \mathbf{R} so that they are separated by $R = |\mathbf{R}|$, there is an exchange interaction between them. The interaction Hamiltonian is,

$$\begin{aligned} \mathcal{H}_{\text{exch}}(R) &= \sum_{f, f'} \sum_{i, i'} V_{f, f'; i, i'}(R) \times \\ &\times X^{f, f'} \hat{\psi}_i^\dagger(\mathbf{R}) \hat{\psi}_i(\mathbf{R}), \end{aligned} \quad (\text{C1})$$

where $X^{f,f'} = |f\rangle\langle f'|$ are Hubbard operators of the localized impurity, $\hat{\psi}_i(\mathbf{R})$ and $\hat{\psi}_i^\dagger(\mathbf{R})$ are annihilation and creation operators of itinerant atoms at position \mathbf{R} with the nuclear magnetic quantum number i . The rate $V_{f,f';i,i'}(R)$ is,

$$V_{f,f';i,i'}(R) = \frac{t_s(R) t_p(R)}{3 \Delta\epsilon} \sum_j C_{J,j;I,i}^{F,f} C_{J,j;I,i'}^{F,f'}. \quad (\text{C2})$$

Here $t_s(R)$ and $t_p(R)$ are given by eq. (26),

$$\Delta\epsilon = \epsilon_{\text{ion}} + \epsilon_{\text{ea}} + \epsilon_g - \epsilon_x = 4.1104 \text{ eV},$$

where $\epsilon_{\text{ion}} = 6.2542 \text{ eV}$ is the ionization energy⁴⁰, $\epsilon_{\text{ea}} = 0.3 \text{ eV}$ is the electron affinity⁴¹ and $\epsilon_x - \epsilon_g = 2.4438 \text{ eV}$ is the excitation energy of the $^3\text{P}_2$ state⁴⁰.

Substituting eq. (C2) into eq. (C1), we get

$$\begin{aligned} \mathcal{H}_{\text{exch}}(R) &= g(R) \sum_j \sum_{f,f'} \sum_{i,i'} C_{J,j;I,i}^{F,f} C_{J,j;I,i'}^{F,f'} \times \\ &\times X^{f,f'} \hat{\psi}_i^\dagger(\mathbf{R}) \hat{\psi}_i(\mathbf{R}), \end{aligned} \quad (\text{C3})$$

where

$$g(R) = \frac{t_s(R) t_p(R)}{3 \Delta\epsilon}. \quad (\text{C4})$$

Appendix D: Derivation of $\delta H_{\beta,\beta'}^{(2)}$, Eq. (31)

Here we consider in turn the various multipole contributions to $\delta H_{\beta,\beta'}^{(2)}$ with $\beta, \beta' = \text{d, q, o}$.

1. Dipole-dipole contribution: The correction $\delta H_{\text{d,d}}^{(2)}$ [eq. (31)] is,

$$\begin{aligned} \delta H_{\text{d,d}}^{(2)} &= -\frac{\lambda_d^2}{D} \sum_{\alpha,\alpha'} \sum_{f,f'} \sum_{i,i'} \sum_{n,n',n''} F_{f,f'}^\alpha F_{f',f'}^{\alpha'} \times \\ &\times X^{f,f'} c_{n,i}^\dagger c_{n',i'} \left(I_{i,i'}^\alpha I_{i'',i'}^{\alpha'} \langle c_{n'',i''}^\dagger c_{n'',i''} \rangle - \right. \\ &\left. - I_{i,i''}^{\alpha'} I_{i',i''}^\alpha \langle c_{n'',i''}^\dagger c_{n'',i''} \rangle \right). \end{aligned} \quad (\text{D1})$$

Here the energy of atoms with harmonic quantum numbers n, n' belong to the reduced energy band, whereas the energy of atoms with the harmonic quantum number n'' is located near the edge of the energy band such that

$$|\epsilon_n|, |\epsilon_{n'}| < D', \quad D' < |\epsilon_{n''}| < D,$$

where $D > D' = D - \delta D$. When $D' \gg T$ (T is the temperature of the gas), we can write

$$\begin{aligned} \langle c_{n'',i''}^\dagger c_{n'',i''} \rangle &= \Theta(\epsilon_{n''} - D) \Theta(-D' - \epsilon_{n''}), \\ \langle c_{n'',i''}^\dagger c_{n'',i''} \rangle &= \Theta(\epsilon_{n''} - D') \Theta(D - \epsilon_{n''}), \end{aligned}$$

where $\Theta(\epsilon)$ is the Heaviside theta function equal to 1 for $\epsilon > 0$, 0 for $\epsilon < 0$ and $\frac{1}{2}$ for $\epsilon = 0$. Thus, the correction

$H_{\text{d,d}}^{(2)}$ can be written as,

$$\begin{aligned} \delta H_{\text{d,d}}^{(2)} &= -\frac{\lambda_d^2 \rho_0 \delta D}{2D} \sum_{\alpha,\alpha'} \sum_{f,f'} \sum_{i,i'} \sum_{n,n'} \left[\hat{F}^\alpha, \hat{F}^{\alpha'} \right]_{f,f'} \times \\ &\times \left[\hat{I}^\alpha, \hat{I}^{\alpha'} \right]_{i,i'} X^{f,f'} c_{n,i}^\dagger c_{n',i'}, \end{aligned} \quad (\text{D2})$$

where

$$[\hat{A}, \hat{B}] = \hat{A}\hat{B} - \hat{B}\hat{A},$$

denotes the commutator of the matrices \hat{A} and \hat{B} . ρ_0 is the density of states of itinerant atoms. Taking into account the property of the Levi-Civita symbols,

$$\sum_{\alpha,\alpha'} \epsilon^{\alpha,\alpha',\alpha_1} \epsilon^{\alpha,\alpha',\alpha'_1} = 2 \delta^{\alpha_1,\alpha'_1}, \quad (\text{D3})$$

we get,

$$\begin{aligned} \delta H_{\text{d,d}}^{(2)} &= -\frac{\lambda_d^2 \rho_0 \delta D}{D} \sum_{\alpha} \sum_{f,f'} \sum_{i,i'} \sum_{n,n'} F_{f,f'}^\alpha I_{i,i'}^\alpha \times \\ &\times X^{f,f'} c_{n,i}^\dagger c_{n',i'}. \end{aligned} \quad (\text{D4})$$

2. Dipole-quadrupole contribution: The correction $\delta H_{\text{d,q}}^{(2)}$ [eq. (31)] is,

$$\begin{aligned} \delta H_{\text{d,q}}^{(2)} &= -\frac{\lambda_d \lambda_q \rho_0 \delta D}{2D} \sum_{\alpha_1,\alpha_2,\alpha'_2} \sum_{f,f'} \sum_{i,i'} \sum_{n,n'} \times \\ &\times \left[\hat{F}^{\alpha_1}, \hat{F}^{\alpha_2,\alpha'_2} \right]_{f,f'} \left[\hat{I}^{\alpha_1}, \hat{I}^{\alpha_2,\alpha'_2} \right]_{i,i'} \times \\ &\times X^{f,f'} c_{n,i}^\dagger c_{n',i'}, \end{aligned} \quad (\text{D5})$$

where ρ_0 is the density of states (23) of itinerant atoms. Taking into account the property (D3) of the Levi-Civita symbols, we get

$$\begin{aligned} \delta H_{\text{d,q}}^{(2)} &= -\frac{12\lambda_d \lambda_q \rho_0 \delta D}{D} \sum_{\alpha,\alpha'} \sum_{f,f'} \sum_{i,i'} \sum_{n,n'} F_{f,f'}^{\alpha,\alpha'} I_{i,i'}^{\alpha,\alpha'} \times \\ &\times X^{f,f'} c_{n,i}^\dagger c_{n',i'}. \end{aligned} \quad (\text{D6})$$

3. Dipole-octupole contribution: The correction $\delta H_{\text{d,o}}^{(2)}$ [eq. (31)] is,

$$\begin{aligned} \delta H_{\text{d,o}}^{(2)} &= -\frac{\lambda_d \lambda_o \rho_0 \delta D}{2D} \sum_{\alpha_1} \sum_{\alpha_2,\alpha'_2,\alpha''_2} \sum_{f,f'} \sum_{i,i'} \sum_{n,n'} \times \\ &\times \left[\hat{F}^{\alpha_1}, \hat{F}^{\alpha_2,\alpha'_2,\alpha''_2} \right]_{f,f'} \left[\hat{I}^{\alpha_1}, \hat{I}^{\alpha_2,\alpha'_2,\alpha''_2} \right]_{i,i'} \times \\ &\times X^{f,f'} c_{n,i}^\dagger c_{n',i'}, \end{aligned} \quad (\text{D7})$$

where ρ_0 is the density of states (23) of itinerant atoms. Taking into account the property (D3) of the Levi-Civita symbols, we get

$$\begin{aligned} \delta H_{\text{d,o}}^{(2)} &= -\frac{18\lambda_d \lambda_o \rho_0 \delta D}{D} \sum_{\alpha,\alpha',\alpha''} \sum_{f,f'} \sum_{i,i'} \sum_{n,n'} \times \\ &\times F_{f,f'}^{\alpha,\alpha',\alpha''} I_{i,i'}^{\alpha,\alpha',\alpha''} X^{f,f'} c_{n,i}^\dagger c_{n',i'}. \end{aligned} \quad (\text{D8})$$

4. Quadrupole-quadrupole contribution: The correction $\delta H_{q,q}^{(2)}$ [eq. (31)] is,

$$\begin{aligned} \delta H_{q,q}^{(2)} = & -\frac{\lambda_q^2 \rho_0 \delta D}{2D} \sum_{\alpha_1, \alpha'_1} \sum_{\alpha_2, \alpha'_2} \sum_{f, f'} \sum_{i, i'} \sum_{n, n'} \\ & \times \left[\hat{F}^{\alpha_1, \alpha'_1}, \hat{F}^{\alpha_2, \alpha'_2} \right]_{f, f'} \left[\hat{I}^{\alpha_1, \alpha'_1}, \hat{I}^{\alpha_2, \alpha'_2} \right]_{i, i'} \times \\ & \times X^{f, f'} c_{n, i}^\dagger c_{n', i'}, \end{aligned} \quad (D9)$$

where ρ_0 is the density of states (23) of itinerant atoms. Taking into account the property (D3) of the Levi-Civita symbols, we get

$$\begin{aligned} \delta H_{q,q}^{(2)} = & -\frac{64\lambda_q^2 \rho_0 \delta D}{9D} \sum_{\alpha, \alpha', \alpha''} \sum_{f, f'} \sum_{i, i'} \sum_{n, n'} \\ & \times F_{f, f'}^{\alpha, \alpha', \alpha''} I_{i, i'}^{\alpha, \alpha', \alpha''} X^{f, f'} c_{n, i}^\dagger c_{n', i'} - \\ & -\frac{9216\lambda_q^2 \rho_0 \delta D}{25D} \sum_{\alpha} \sum_{f, f'} \sum_{i, i'} \sum_{n, n'} \\ & \times F_{f, f'}^{\alpha} I_{i, i'}^{\alpha} X^{f, f'} c_{n, i}^\dagger c_{n', i'}. \end{aligned} \quad (D10)$$

5. Quadrupole-octupole contribution: The correction $\delta H_{q,o}^{(2)}$ [eq. (31)] is,

$$\begin{aligned} \delta H_{q,o}^{(2)} = & -\frac{\lambda_q \lambda_o \rho_0 \delta D}{2D} \sum_{\alpha_1, \alpha'_1} \sum_{\alpha_2, \alpha'_2, \alpha''_2} \sum_{f, f'} \sum_{i, i'} \sum_{n, n'} \\ & \times \left[\hat{F}^{\alpha_1, \alpha'_1}, \hat{F}^{\alpha_2, \alpha'_2, \alpha''_2} \right]_{f, f'} \times \\ & \times \left[\hat{I}^{\alpha_1, \alpha'_1}, \hat{I}^{\alpha_2, \alpha'_2, \alpha''_2} \right]_{i, i'} \times \\ & \times X^{f, f'} c_{n, i}^\dagger c_{n', i'}, \end{aligned} \quad (D11)$$

where ρ_0 is the density of states (23) of itinerant atoms. Then eq. (D11) takes the form,

$$\begin{aligned} \delta H_{q,o}^{(2)} = & -\frac{1458\lambda_q \lambda_o}{5D} \sum_{\alpha, \alpha'} \sum_{f, f'} \sum_{i, i'} \sum_{n, n'} F_{f, f'}^{\alpha, \alpha'} I_{i', i}^{\alpha', \alpha} \times \\ & \times X^{f, f'} c_{n', i'}^\dagger c_{n, i}. \end{aligned} \quad (D12)$$

6. Octupole-octupole contribution: The correction $\delta H_{o,o}^{(2)}$ [eq. (31)] is,

$$\begin{aligned} \delta H_{o,o}^{(2)} = & -\frac{\lambda_q \lambda_o \rho_0 \delta D}{2D} \sum_{\alpha_1, \alpha'_1, \alpha''_1} \sum_{\alpha_2, \alpha'_2, \alpha''_2} \sum_{f, f'} \sum_{i, i'} \sum_{n, n'} \\ & \times \left[\hat{F}^{\alpha_1, \alpha'_1, \alpha''_1}, \hat{F}^{\alpha_2, \alpha'_2, \alpha''_2} \right]_{f, f'} \times \\ & \times \left[\hat{I}^{\alpha_1, \alpha'_1, \alpha''_1}, \hat{I}^{\alpha_2, \alpha'_2, \alpha''_2} \right]_{i, i'} \times \\ & \times X^{f, f'} c_{n, i}^\dagger c_{n', i'}, \end{aligned} \quad (D13)$$

where ρ_0 is the density of states (23) of itinerant atoms.

Then eq. (D13) takes the form,

$$\begin{aligned} \delta H_{o,o}^{(2)} = & -\frac{1469664\lambda_o^2 \rho_0 \delta D}{25D} \sum_{\alpha} \sum_{f, f'} \sum_{i, i'} \sum_{n, n'} F_{f, f'}^{\alpha} I_{i', i}^{\alpha} \times \\ & \times X^{f, f'} c_{n', i'}^\dagger c_{n, i} + \\ & +\frac{306\lambda_o^2 \rho_0 \delta D}{5D} \sum_{\alpha, \alpha', \alpha''} \sum_{f, f'} \sum_{i, i'} \sum_{n, n'} \times \\ & \times F_{f, f'}^{\alpha, \alpha', \alpha''} I_{i', i}^{\alpha'', \alpha', \alpha} X^{f, f'} c_{n', i'}^\dagger c_{n, i}. \end{aligned} \quad (D14)$$

Appendix E: Derivation of δE , Eq. (37)

The second order correction to the energy is illustrated by the diagrams displayed in Fig. 6. is decomposed into its multipole components as,

$$\delta E = \delta E_d + \delta E_q + \delta E_o. \quad (E1)$$

Here δE_d , δE_q and δE_o are dipole, quadrupole and octupole contributions to δE , given explicitly as,

$$\begin{aligned} \delta E_d = & -\lambda_d^2 \frac{E}{D^2} \sum_{f, f'} X^{f, f'} \sum_{\alpha_1, \alpha_2} \left(\hat{F}^{\alpha_1} \hat{F}^{\alpha_2} \right)_{f, f'} \times \\ & \times \text{Tr} \left(\hat{I}^{\alpha_1} \hat{I}^{\alpha_2} \right) 2\rho_0^2 D \delta D, \end{aligned} \quad (E2a)$$

$$\begin{aligned} \delta E_q = & -\lambda_q^2 \frac{E}{D^2} \sum_{f, f'} X^{f, f'} \times \\ & \times \sum_{\alpha_1, \alpha'_1} \sum_{\alpha_2, \alpha'_2} \left(\hat{F}^{\alpha_1, \alpha'_1} \hat{F}^{\alpha_2, \alpha'_2} \right)_{f, f'} \times \\ & \times \text{Tr} \left(\hat{I}^{\alpha_1, \alpha'_1} \hat{I}^{\alpha_2, \alpha'_2} \right) 2\rho_0^2 D \delta D, \end{aligned} \quad (E2b)$$

$$\begin{aligned} \delta E_o = & -\lambda_o^2 \frac{E}{D^2} \sum_{f, f'} X^{f, f'} \sum_{\alpha_1, \alpha'_1, \alpha''_1} \sum_{\alpha_2, \alpha'_2, \alpha''_2} \\ & \times \left(\hat{F}^{\alpha_1, \alpha'_1, \alpha''_1} \hat{F}^{\alpha_2, \alpha'_2, \alpha''_2} \right)_{f, f'} \times \\ & \times \text{Tr} \left(\hat{I}^{\alpha_1, \alpha'_1, \alpha''_1} \hat{I}^{\alpha_2, \alpha'_2, \alpha''_2} \right) 2\rho_0^2 D \delta D, \end{aligned} \quad (E2c)$$

We consider dipole, quadrupole and octupole contributions to δE in turn.

1. Dipole contribution: The trace of the product of two spin matrices is,

$$\sum_{i_1, i_2} I_{i_1, i_2}^{\alpha_1} I_{i_2, i_1}^{\alpha_2} = \frac{1}{3} I(I+1)(2I+1) \delta^{\alpha_1, \alpha_2}. \quad (E3)$$

Using eq. (E3), we can write

$$\sum_{\alpha} \sum_{f_1} F_{f, f_1}^{\alpha} F_{f_1, f'}^{\alpha} = F(F+1) \delta_{f, f'}. \quad (E4)$$

Finally, the dipole contribution to the self energy is,

$$\delta E_d = -\frac{2\delta D}{3D} E \Lambda_d^2 F(F+1)I(I+1)(2I+1).$$

Taking into account that $F = \frac{3}{2}$ and $I = \frac{5}{2}$, we get

$$\delta E_d = -\frac{525}{4} \frac{\delta D}{D} E \Lambda_d^2. \quad (\text{E5})$$

2. Quadrupole contribution: The trace of the product of two quadrupole matrices is,

$$\sum_{i_1, i_2} I_{i_1, i_2}^{\alpha_1, \alpha'_1} I_{i_2, i_1}^{\alpha_2, \alpha'_2} = -\frac{112}{3} \left\{ 2 \delta_{\alpha_1, \alpha'_1} \delta_{\alpha_2, \alpha'_2} - 3 [\delta_{\alpha_1, \alpha_2} \delta_{\alpha'_1, \alpha'_2} + \delta_{\alpha_1, \alpha'_2} \delta_{\alpha'_1, \alpha_2}] \right\}. \quad (\text{E6})$$

Using eq. (E6), we can write

$$\sum_{\alpha_1, \alpha'_1} \sum_{\alpha_2, \alpha'_2} \hat{F}^{\alpha_1, \alpha'_1} \hat{F}^{\alpha_2, \alpha'_2} \text{Tr}(\hat{F}^{\alpha_1, \alpha'_1} \hat{F}^{\alpha_2, \alpha'_2}) = 6720 \hat{1}_4, \quad (\text{E7})$$

where $\hat{1}_4$ is the 4×4 identity matrix.

Finally, quadrupole contribution to the self energy is,

$$\delta E_q = -13440 \frac{\delta D}{D} E \Lambda_q^2. \quad (\text{E8})$$

3. Octupole contribution: The trace of the product of two quadrupole matrices is,

$$\sum_{\alpha_1, \alpha'_1, \alpha''_1} \sum_{\alpha_2, \alpha'_2, \alpha''_2} \hat{F}^{\alpha_1, \alpha'_1, \alpha''_1} \hat{F}^{\alpha_2, \alpha'_2, \alpha''_2} \times \text{Tr}(\hat{F}^{\alpha_1, \alpha'_1, \alpha''_1} \hat{F}^{\alpha_2, \alpha'_2, \alpha''_2}) = 1653372 \hat{1}_4, \quad (\text{E9})$$

where $\hat{1}_4$ is the 4×4 identity matrix.

Finally, octupole contribution to the self energy is,

$$\delta E_o = -3306744 \frac{\delta D}{D} E \Lambda_q^2. \quad (\text{E10})$$

Finally, the second order correction to the energy is,

$$\delta E = -\frac{\delta D}{D} E \left\{ \frac{525}{4} \Lambda_d^2 + 13440 \Lambda_q^2 + 3306744 \Lambda_o^2 \right\}. \quad (\text{E11})$$

Appendix F: Derivation of $\delta H_{\beta, \beta', \beta}^{(3)}$, Eq. (39)

We consider $\delta H_{\beta', \beta, \beta'}^{(3)}$ for $\beta, \beta' = d, q, o$, in turn.

1. Dipole-dipole contribution: The correction $\delta H_{d, d, d}^{(3)}$ is,

$$\delta H_{d, d, d}^{(3)} = \frac{2\lambda_d^3 \rho_0^2 \delta D}{D} \sum_{\alpha_1, \alpha_2, \alpha_3} \sum_{f, f'} \left(\hat{F}^{\alpha_1} \hat{F}^{\alpha_2} \hat{F}^{\alpha_3} \right)_{f, f'} \times X^{f, f'} \sum_{i, i'} \sum_{n, n'} I_{i, i'}^{\alpha_2} c_{n, i}^\dagger c_{n', i'} \times \text{Tr}(\hat{F}^{\alpha_1} \hat{F}^{\alpha_3}). \quad (\text{F1})$$

In order to simplify the expression in the right hand side of eq. (F1), we use the following equalities,

$$\begin{aligned} \text{Tr}(\hat{F}^{\alpha_1} \hat{F}^{\alpha_3}) &= \frac{1}{3} I(I+1)(2I+1) = \\ &= \frac{35}{2} \delta_{\alpha_1, \alpha_3}, \end{aligned} \quad (\text{F2})$$

$$\begin{aligned} \sum_{\alpha_1} \hat{F}^{\alpha_1} \hat{F}^{\alpha_2} \hat{F}^{\alpha_1} &= (F(F+1) - 1) \hat{F}^{\alpha_2} = \\ &= \frac{11}{4} \hat{F}^{\alpha_2}. \end{aligned} \quad (\text{F3})$$

Then the dipole-dipole contribution takes the form,

$$\begin{aligned} \delta H_{d, d, d}^{(3)} &= \frac{385}{4} \frac{\lambda_d^3 \rho_0^2 \delta D}{D} \sum_{\alpha} \sum_{f, f'} \sum_{i, i'} \sum_{n, n'} \\ &\times F_{f, f'}^\alpha I_{i, i'}^\alpha X^{f, f'} c_{n, i}^\dagger c_{n', i'}. \end{aligned} \quad (\text{F4})$$

2. Dipole-quadrupole contribution: The correction $\delta H_{q, d, q}^{(3)}$ is,

$$\begin{aligned} \delta H_{q, d, q}^{(3)} &= \frac{2\lambda_d \lambda_q^2 \rho_0^2 \delta D}{D} \sum_{\alpha_1, \alpha'_1} \sum_{\alpha_2} \sum_{\alpha_3, \alpha'_3} \sum_{f, f'} \\ &\times \left(\hat{F}^{\alpha_1, \alpha'_1} \hat{F}^{\alpha_2} \hat{F}^{\alpha_3, \alpha'_3} \right)_{f, f'} \times \\ &\times X^{f, f'} \sum_{i, i'} \sum_{n, n'} I_{i, i'}^{\alpha_2} c_{n, i}^\dagger c_{n', i'} \times \\ &\times \text{Tr}(\hat{F}^{\alpha_1, \alpha'_1} \hat{F}^{\alpha_3, \alpha'_3}). \end{aligned} \quad (\text{F5})$$

Using eqs. (E6) and (E7), we can write

$$\begin{aligned} \sum_{\alpha_1, \alpha'_1} \sum_{\alpha_3, \alpha'_3} \hat{F}^{\alpha_1, \alpha'_1} \hat{F}^{\alpha_2} \hat{F}^{\alpha_3, \alpha'_3} \text{Tr}(\hat{F}^{\alpha_1, \alpha'_1} \hat{F}^{\alpha_3, \alpha'_3}) &= \\ &= 1344 \hat{F}^{\alpha_2}. \end{aligned}$$

Then the dipole-quadrupole contribution can be written as,

$$\begin{aligned} \delta H_{q, d, q}^{(3)} &= 2688 \frac{\lambda_d \lambda_q^2 \rho_0^2 \delta D}{D} \sum_{\alpha} \sum_{f, f'} \sum_{i, i'} \sum_{n, n'} \\ &\times F_{f, f'}^\alpha I_{i, i'}^\alpha X^{f, f'} c_{n, i}^\dagger c_{n', i'}. \end{aligned} \quad (\text{F6})$$

3. Dipole-octupole contribution: The correction $\delta H_{o, d, o}^{(3)}$ is,

$$\begin{aligned} \delta H_{o, d, o}^{(3)} &= \frac{2\lambda_d \lambda_o^2 \rho_0^2 \delta D}{D} \sum_{\alpha_1, \alpha'_1, \alpha''_1} \sum_{\alpha_2} \sum_{\alpha_3, \alpha'_3, \alpha''_3} \sum_{f, f'} \\ &\times \left(\hat{F}^{\alpha_1, \alpha'_1, \alpha''_1} \hat{F}^{\alpha_2} \hat{F}^{\alpha_3, \alpha'_3, \alpha''_3} \right)_{f, f'} \times \\ &\times X^{f, f'} \sum_{i, i'} \sum_{n, n'} I_{i, i'}^{\alpha_2} c_{n, i}^\dagger c_{n', i'} \times \\ &\times \text{Tr}(\hat{F}^{\alpha_1, \alpha'_1, \alpha''_1} \hat{F}^{\alpha_3, \alpha'_3, \alpha''_3}). \end{aligned} \quad (\text{F7})$$

Equation (F7) can be simplified by using eq. (E9),

$$\begin{aligned} & \sum_{\alpha_1, \alpha'_1, \alpha''_1} \sum_{\alpha_3, \alpha'_3, \alpha''_3} \hat{F}^{\alpha_1, \alpha'_1, \alpha''_1} \hat{F}^{\alpha_2} \hat{F}^{\alpha_3, \alpha'_3, \alpha''_3} \times \\ & \times \text{Tr} \left(\hat{F}^{\alpha_1, \alpha'_1, \alpha''_1} \hat{F}^{\alpha_3, \alpha'_3, \alpha''_3} \right) = \\ & = -\frac{4960116}{5} \hat{F}^{\alpha_2}. \end{aligned}$$

Then the dipole-quadrupole contribution can be written as,

$$\begin{aligned} \delta H_{o,d,o}^{(3)} &= -\frac{9920232}{5} \frac{\lambda_d \lambda_o^2 \rho_0^2 \delta D}{D} \sum_{\alpha} \sum_{f, f'} \sum_{i, i'} \sum_{n, n'} \\ & \times F_{f, f'}^{\alpha} I_{i, i'}^{\alpha} X^{f, f'} c_{n, i}^{\dagger} c_{n', i'}. \end{aligned} \quad (\text{F8})$$

4. Quadrupole-dipole contribution: The correction $\delta H_{d,q,d}^{(3)}$ is,

$$\begin{aligned} \delta H_{d,q,d}^{(3)} &= \frac{2\lambda_q \lambda_d^2 \rho_0^2 \delta D}{D} \sum_{\alpha_1} \sum_{\alpha_2, \alpha'_2} \sum_{\alpha_3} \sum_{f, f'} \\ & \times \left(\hat{F}^{\alpha_1} \hat{F}^{\alpha_2, \alpha'_2} \hat{F}^{\alpha_3} \right)_{f, f'} \times \\ & \times X^{f, f'} \sum_{i, i'} \sum_{n, n'} I_{i, i'}^{\alpha_2, \alpha'_2} c_{n, i}^{\dagger} c_{n', i'} \times \\ & \times \text{Tr} \left(\hat{I}^{\alpha_1} \hat{I}^{\alpha_3} \right). \end{aligned} \quad (\text{F9})$$

In order to simplify eq. (F9), we use eq. (E3) and the following equality,

$$\sum_{\alpha} \hat{F}^{\alpha} \hat{F}^{\alpha_2, \alpha'_2} \hat{F}^{\alpha} = \frac{3}{4} \hat{F}^{\alpha_2, \alpha'_2}.$$

Then the quadrupole-dipole contribution can be written as,

$$\begin{aligned} \delta H_{d,q,d}^{(3)} &= \frac{105}{4} \frac{\lambda_q \lambda_d^2 \rho_0^2 \delta D}{D} \sum_{\alpha} \sum_{f, f'} \sum_{i, i'} \sum_{n, n'} \\ & \times F_{f, f'}^{\alpha} I_{i, i'}^{\alpha} X^{f, f'} c_{n, i}^{\dagger} c_{n', i'}. \end{aligned} \quad (\text{F10})$$

5. Quadrupole-quadrupole contribution: The correction $\delta H_{q,q,q}^{(3)}$ is,

$$\begin{aligned} \delta H_{q,q,q}^{(3)} &= \frac{2\lambda_q^3 \rho_0^2 \delta D}{D} \sum_{\alpha_1, \alpha'_1} \sum_{\alpha_2, \alpha'_2} \sum_{\alpha_3, \alpha'_3} \sum_{f, f'} \\ & \times \left(\hat{F}^{\alpha_1, \alpha'_1} \hat{F}^{\alpha_2, \alpha'_2} \hat{F}^{\alpha_3, \alpha'_3} \right)_{f, f'} \times \\ & \times X^{f, f'} \sum_{i, i'} \sum_{n, n'} I_{i, i'}^{\alpha_2, \alpha'_2} c_{n, i}^{\dagger} c_{n', i'} \times \\ & \times \text{Tr} \left(\hat{I}^{\alpha_1, \alpha'_1} \hat{I}^{\alpha_3, \alpha'_3} \right). \end{aligned} \quad (\text{F11})$$

Using eqs. (E6) and (E7), we can write

$$\begin{aligned} & \sum_{\alpha_1, \alpha'_1} \sum_{\alpha_3, \alpha'_3} \hat{F}^{\alpha_1, \alpha'_1} \hat{F}^{\alpha_2, \alpha'_2} \hat{F}^{\alpha_3, \alpha'_3} \text{Tr} \left(\hat{I}^{\alpha_1, \alpha'_1} \hat{I}^{\alpha_3, \alpha'_3} \right) = \\ & = -4032 \hat{F}^{\alpha_2, \alpha'_2}. \end{aligned}$$

Then $\delta H_{q,q,q}^{(3)}$ takes the form,

$$\begin{aligned} \delta H_{q,q,q}^{(3)} &= -8064 \frac{\lambda_q^3 \rho_0^2 \delta D}{D} \sum_{\alpha, \alpha'} \sum_{f, f'} \sum_{i, i'} \sum_{n, n'} \\ & \times F_{f, f'}^{\alpha, \alpha'} I_{i, i'}^{\alpha_2, \alpha'_2} X^{f, f'} c_{n, i}^{\dagger} c_{n', i'}. \end{aligned} \quad (\text{F12})$$

6. Quadrupole-octupole contribution: The correction $\delta H_{o,q,o}^{(3)}$ is,

$$\begin{aligned} \delta H_{o,q,o}^{(3)} &= \frac{2\lambda_q \lambda_o^2 \rho_0^2 \delta D}{D} \sum_{\alpha_1, \alpha'_1, \alpha''_1} \sum_{\alpha_2, \alpha'_2} \sum_{\alpha_3, \alpha'_3, \alpha''_3} \sum_{f, f'} \\ & \times \left(\hat{F}^{\alpha_1, \alpha'_1, \alpha''_1} \hat{F}^{\alpha_2, \alpha'_2} \hat{F}^{\alpha_3, \alpha'_3, \alpha''_3} \right)_{f, f'} \times \\ & \times X^{f, f'} \sum_{i, i'} \sum_{n, n'} I_{i, i'}^{\alpha_2, \alpha'_2} c_{n, i}^{\dagger} c_{n', i'} \times \\ & \times \text{Tr} \left(\hat{I}^{\alpha_1, \alpha'_1, \alpha''_1} \hat{I}^{\alpha_3, \alpha'_3, \alpha''_3} \right). \end{aligned} \quad (\text{F13})$$

In order to simplify eq. (F13), we use the following equality,

$$\begin{aligned} & \sum_{\alpha_1, \alpha'_1, \alpha''_1} \sum_{\alpha_3, \alpha'_3, \alpha''_3} \hat{F}^{\alpha_1, \alpha'_1, \alpha''_1} \hat{F}^{\alpha_2, \alpha'_2} \hat{F}^{\alpha_3, \alpha'_3, \alpha''_3} \times \\ & \times \text{Tr} \left(\hat{I}^{\alpha_1, \alpha'_1, \alpha''_1} \hat{I}^{\alpha_3, \alpha'_3, \alpha''_3} \right) = \\ & = \frac{1153372}{5} \hat{F}^{\alpha_2, \alpha'_2}. \end{aligned}$$

Then eq. (F13) takes the form,

$$\begin{aligned} \delta H_{o,q,o}^{(3)} &= \frac{2306744}{5} \frac{\lambda_q \lambda_o^2 \rho_0^2 \delta D}{D} \sum_{\alpha, \alpha'} \sum_{f, f'} \sum_{i, i'} \sum_{n, n'} \\ & \times F_{f, f'}^{\alpha, \alpha'} I_{i, i'}^{\alpha} X^{f, f'} c_{n, i}^{\dagger} c_{n', i'}. \end{aligned} \quad (\text{F14})$$

7. Octupole-dipole contribution: The correction $\delta H_{d,o,d}^{(3)}$ is,

$$\begin{aligned} \delta H_{d,o,d}^{(3)} &= \frac{2\lambda_o \lambda_d^2 \rho_0^2 \delta D}{D} \sum_{\alpha_1} \sum_{\alpha_2, \alpha'_2, \alpha''_2} \sum_{\alpha_3} \sum_{f, f'} \\ & \times \left(\hat{F}^{\alpha_1} \hat{F}^{\alpha_2, \alpha'_2, \alpha''_2} \hat{F}^{\alpha_3} \right)_{f, f'} \times \\ & \times X^{f, f'} \sum_{i, i'} \sum_{n, n'} I_{i, i'}^{\alpha_2, \alpha'_2, \alpha''_2} c_{n, i}^{\dagger} c_{n', i'} \times \\ & \times \text{Tr} \left(\hat{I}^{\alpha_1} \hat{I}^{\alpha_3} \right). \end{aligned} \quad (\text{F15})$$

In order to simplify eq. (F15), we use the following equality,

$$\begin{aligned} & \sum_{\alpha_1, \alpha_3} \hat{F}^{\alpha_1} \hat{F}^{\alpha_2, \alpha'_2, \alpha''_2} \hat{F}^{\alpha_3} \text{Tr} \left(\hat{I}^{\alpha_1} \hat{I}^{\alpha_3} \right) = \\ & = -\frac{315}{8} \hat{F}^{\alpha_2, \alpha'_2, \alpha''_2}. \end{aligned}$$

Then the octupole-dipole contribution can be written as,

$$\delta H_{d,o,d}^{(3)} = -\frac{315}{4} \frac{\lambda_o \lambda_d^2 \rho_0^2 \delta D}{D} \sum_{\alpha,\alpha',\alpha''} \sum_{f,f'} \sum_{i,i'} \sum_{n,n'} \times F_{f,f'}^{\alpha,\alpha',\alpha''} I_{i,i'}^{\alpha,\alpha',\alpha''} X^{f,f'} c_{n,i}^\dagger c_{n',i'}. \quad (\text{F16})$$

8. Octupole-quadrupole contribution: The correction $\delta H_{q,o,q}^{(3)}$ is,

$$\delta H_{q,o,q}^{(3)} = \frac{2\lambda_o \lambda_q^2 \rho_0^2 \delta D}{D} \sum_{\alpha_1,\alpha'_1} \sum_{\alpha_2,\alpha'_2,\alpha''_2} \sum_{\alpha_3,\alpha'_3} \sum_{f,f'} \times \left(\hat{F}^{\alpha_1,\alpha'_1} \hat{F}^{\alpha_2,\alpha'_2,\alpha''_2} \hat{F}^{\alpha_3,\alpha'_3} \right)_{f,f'} \times X^{f,f'} \sum_{i,i'} \sum_{n,n'} I_{i,i'}^{\alpha_2,\alpha'_2,\alpha''_2} c_{n,i}^\dagger c_{n',i'} \times \text{Tr} \left(\hat{I}^{\alpha_1,\alpha'_1} \hat{I}^{\alpha_3,\alpha'_3} \right). \quad (\text{F17})$$

Using eqs. (E6) and (E7), we can write

$$\sum_{\alpha_1,\alpha'_1} \sum_{\alpha_3,\alpha'_3} \hat{F}^{\alpha_1,\alpha'_1} \hat{F}^{\alpha_2,\alpha'_2,\alpha''_2} \hat{F}^{\alpha_3,\alpha'_3} \text{Tr} \left(\hat{I}^{\alpha_1,\alpha'_1} \hat{I}^{\alpha_3,\alpha'_3} \right) = 1344 \hat{F}^{\alpha_2,\alpha'_2,\alpha''_2}.$$

Then $\delta H_{q,o,q}^{(3)}$ takes the form,

$$\delta H_{q,o,q}^{(3)} = 2688 \frac{\lambda_o \lambda_q^2 \rho_0^2 \delta D}{D} \sum_{\alpha,\alpha',\alpha''} \sum_{f,f'} \sum_{i,i'} \sum_{n,n'} \times F_{f,f'}^{\alpha,\alpha',\alpha''} I_{i,i'}^{\alpha,\alpha',\alpha''} X^{f,f'} c_{n,i}^\dagger c_{n',i'}. \quad (\text{F18})$$

9. Octupole-octupole contribution: The correction $\delta H_{o,o,o}^{(3)}$ is,

$$\delta H_{o,o,o}^{(3)} = \frac{2\lambda_o^3 \rho_0^2 \delta D}{D} \sum_{\alpha_1,\alpha'_1,\alpha''_1} \sum_{\alpha_2,\alpha'_2,\alpha''_2} \sum_{\alpha_3,\alpha'_3,\alpha''_3} \sum_{f,f'} \times \left(\hat{F}^{\alpha_1,\alpha'_1,\alpha''_1} \hat{F}^{\alpha_2,\alpha'_2,\alpha''_2} \hat{F}^{\alpha_3,\alpha'_3,\alpha''_3} \right)_{f,f'} \times X^{f,f'} \sum_{i,i'} \sum_{n,n'} I_{i,i'}^{\alpha_2,\alpha'_2,\alpha''_2} c_{n,i}^\dagger c_{n',i'} \times \text{Tr} \left(\hat{I}^{\alpha_1,\alpha'_1,\alpha''_1} \hat{I}^{\alpha_3,\alpha'_3,\alpha''_3} \right). \quad (\text{F19})$$

In order to simplify eq. (F19), we use the following equality,

$$\sum_{\alpha_1,\alpha'_1,\alpha''_1} \sum_{\alpha_3,\alpha'_3,\alpha''_3} \hat{F}^{\alpha_1,\alpha'_1,\alpha''_1} \hat{F}^{\alpha_2,\alpha'_2,\alpha''_2} \hat{F}^{\alpha_3,\alpha'_3,\alpha''_3} \times \text{Tr} \left(\hat{I}^{\alpha_1,\alpha'_1,\alpha''_1} \hat{I}^{\alpha_3,\alpha'_3,\alpha''_3} \right) = -\frac{236196}{5} \hat{F}^{\alpha_2,\alpha'_2,\alpha''_2}.$$

Then eq. (F19) takes the form,

$$\delta H_{o,o,o}^{(3)} = -\frac{472392}{5} \frac{\lambda_o^3 \rho_0^2 \delta D}{D} \sum_{\alpha,\alpha',\alpha''} \sum_{f,f'} \sum_{i,i'} \sum_{n,n'} \times F_{f,f'}^{\alpha,\alpha',\alpha''} I_{i,i'}^{\alpha,\alpha',\alpha''} X^{f,f'} c_{n,i}^\dagger c_{n',i'}. \quad (\text{F20})$$

Appendix G: Eigenfunctions and Eigenenergies of the Dipole-Dipole, Quadrupole-Quadrupole and Octupole-Octupole Interactions

Appendix G main points The dipole-dipole, quadrupole-quadrupole and octupole-octupole Hamiltonians are defined in Eqs. (G1, G5, G8) respectively. Their eigenfunctions and eigenenergies, required for the calculations of the exchange constants, are explicitly elucidated in this Appendix.

Consider four atoms, such that one atom (an ‘‘impurity atom’’) has spin $F = \frac{3}{2}$ and the three other atoms (‘‘itinerant atoms’’) have spin $I = \frac{5}{2}$. The interaction between the itinerant atoms and the impurity is dipole-dipole, quadrupole-quadrupole and octupole-octupole interactions. We derive here eigenfunctions and corresponding eigenenergies of the Hamiltonians of the dipole-dipole, quadrupole-quadrupole and octupole-octupole interactions, in turn.

1. Eigenfunctions of the Dipole-Dipole Interaction

The Hamiltonian of the dipole-dipole interaction between the atoms is,

$$\mathcal{H}_d = \lambda_d \left(\hat{\mathbf{F}} \cdot \hat{\mathbf{S}} \right), \quad (\text{G1})$$

where $\hat{\mathbf{F}}$ is a vector of the spin- $\frac{3}{2}$ operators, $\hat{\mathbf{S}} = \hat{\mathbf{I}}_1 + \hat{\mathbf{I}}_2 + \hat{\mathbf{I}}_3$, where $\hat{\mathbf{I}}_a$ ($a = 1, 2, 3$) is a vector of the spin- $\frac{5}{2}$ operators.

Note that \mathcal{H}_d can be expressed in terms of the two-atomic spin $\hat{\mathbf{L}}$,

$$\mathcal{H}_d = \frac{\lambda_d}{2} \left(\hat{\mathbf{L}}^2 - F(F+1) - S(S+1) \right), \quad (\text{G2})$$

where

$$\hat{\mathbf{L}} = \hat{\mathbf{F}} + \hat{\mathbf{S}},$$

Eq. (G2) shows that \mathcal{H}_d commutes with $\hat{\mathbf{L}}^2$, $\hat{\mathbf{F}}^2$ and $\hat{\mathbf{S}}^2$. In addition, \mathcal{H}_d commutes with $\hat{\mathbf{L}}^z$, but neither with $\hat{\mathbf{F}}^z$ nor $\hat{\mathbf{S}}^z$. The eigenfunctions of \mathcal{H}_d , $|L, L_z\rangle$, are defined as

$$\begin{aligned} \hat{\mathbf{L}}^2 |L, L_z\rangle &= L(L+1) |L, L_z\rangle, \\ \hat{\mathbf{L}}^z |L, L_z\rangle &= L_z |L, L_z\rangle, \end{aligned}$$

where $L = 3, 4, 5, 6$. The corresponding eigenvalues of \mathcal{H}_d are,

$$\mathcal{E}_L^{(d)} = \lambda_d \mathcal{D}_L, \quad (\text{G3})$$

where

$$\mathcal{D}_L = \frac{1}{2} \left(L(L+1) - F(F+1) - S(S+1) \right). \quad (\text{G4})$$

When $\lambda_d > 0$, the lowest energy level has maximal value of S and minimal value of L . For $I = \frac{5}{2}$, this is the level $S = \frac{9}{2}$ and $L = 3$ (see discussions in Sec. X). Therefore, we conclude that the interaction is antiferromagnetic.

2. Eigenfunctions of the Quadrupole-Quadrupole Interaction

The Hamiltonian of the quadrupole-quadrupole interaction between the atoms is,

$$\mathcal{H}_q = \lambda_q \sum_{\alpha, \alpha'} \hat{F}^{\alpha, \alpha'} \hat{S}^{\alpha, \alpha'}, \quad (\text{G5})$$

where $\hat{F}^{\alpha, \alpha'}$ or $\hat{S}_a^{\alpha, \alpha'}$ is a quadrupole operator for the atom with spin- $\frac{3}{2}$ or spin- $\frac{9}{2}$,

$$\begin{aligned} \hat{F}^{\alpha, \alpha'} &= \hat{F}^\alpha \hat{F}^{\alpha'} + \hat{F}^{\alpha'} \hat{F}^\alpha - \frac{2}{3} F(F+1) \delta_{\alpha, \alpha'}, \\ \hat{S}^{\alpha, \alpha'} &= \hat{S}^\alpha \hat{S}^{\alpha'} + \hat{S}^{\alpha'} \hat{S}^\alpha - \frac{2}{3} S(S+1) \delta_{\alpha, \alpha'}. \end{aligned}$$

\mathcal{H}_q can be expressed in terms of $(\hat{\mathbf{F}} \cdot \hat{\mathbf{S}})$ as,

$$\mathcal{H}_q = \lambda_q \left\{ 4 (\hat{\mathbf{F}} \cdot \hat{\mathbf{S}})^2 + 2 (\hat{\mathbf{F}} \cdot \hat{\mathbf{S}}) - \frac{4}{3} F(F+1) S(S+1) \right\}.$$

Eigenfunctions of \mathcal{H}_q are $|L, L_z\rangle$. Corresponding eigenenergies are,

$$\mathcal{E}_L^{(q)} = \lambda_q \mathcal{Q}_L, \quad (\text{G6})$$

where

$$\mathcal{Q}_L = 4 \mathcal{D}_L^2 + 2 \mathcal{D}_L - \frac{4}{3} F(F+1) S(S+1),$$

\mathcal{D}_L is given by eq. (G4).

The spin L takes the values $L = 3, 4, 5, 6$. Corresponding energies are,

$$\begin{aligned} \mathcal{E}_3^{(q)} &= 132 \lambda_q, \\ \mathcal{E}_4^{(q)} &= -60 \lambda_q, \\ \mathcal{E}_5^{(q)} &= -120 \lambda_q, \\ \mathcal{E}_6^{(q)} &= 72 \lambda_q. \end{aligned} \quad (\text{G7})$$

It is seen that when $\lambda_q < 0$, the lowest energy level is the $L = 3$ energy level. For $\lambda_q > 0$, the lowest energy level is the $L = 5$ energy level.

3. Eigenfunctions of the Octupole-Octupole Interaction

The Hamiltonian of the octupole-octupole interaction between the impurity and the itinerant atoms is,

$$\mathcal{H}_o = \lambda_o \sum_{\alpha, \alpha', \alpha''} \hat{F}^{\alpha, \alpha', \alpha''} \hat{S}^{\alpha, \alpha', \alpha''}, \quad (\text{G8})$$

where $\hat{F}^{\alpha, \alpha', \alpha''}$ or $\hat{S}^{\alpha, \alpha', \alpha''}$ is an octupole operator for the atom with spin- $\frac{3}{2}$ or spin- $\frac{9}{2}$, see eq. (B4).

Substituting eq. (B4) into eq. (G8), we get

$$\begin{aligned} \mathcal{H}_o &= \lambda_o \left\{ 36 (\hat{\mathbf{F}} \cdot \hat{\mathbf{I}})^3 + 72 (\hat{\mathbf{F}} \cdot \hat{\mathbf{I}})^2 + 12 (\hat{\mathbf{F}} \cdot \hat{\mathbf{I}}) - \right. \\ &\quad \left. - \frac{12}{5} (3F(F+1) - 1)(3S(S+1) - 1) (\hat{\mathbf{F}} \cdot \hat{\mathbf{I}}) - \right. \\ &\quad \left. - 18 F(F+1) S(S+1) \right\}. \end{aligned}$$

The spin L takes the values $L = 3, 4, 5, 6$. Corresponding energies are,

$$\begin{aligned} \mathcal{E}_3^{(o)} &= -\frac{11088}{5} \lambda_o, \\ \mathcal{E}_4^{(o)} &= \frac{22368}{5} \lambda_o, \\ \mathcal{E}_5^{(o)} &= -\frac{14787}{5} \lambda_o, \\ \mathcal{E}_6^{(o)} &= 2997 \lambda_o. \end{aligned} \quad (\text{G9})$$

It is seen that when $\lambda_o < 0$, the lowest energy level is the $L = 4$ energy level. When $\lambda_o > 0$, the lowest energy level is the $L = 5$ energy level.

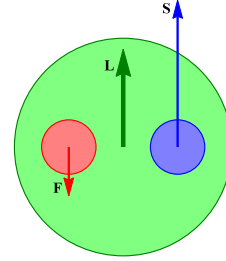


FIG. 13: (Color online) Impurity atom with spin F (red disk), itinerant atoms with total spin S (blue disk) creating a cloud screening the spin of the impurity. The spin of the “dressed” impurity is L .

Screening of the impurity spin by a cloud of itinerant atoms is illustrated in Fig. 13. Here the red disk denotes the impurity atom with spin F , the blue disk denotes a cloud of itinerant atoms with the total spin S . The green arrow is a “dressed” spin of the impurity $\mathbf{L} = \mathbf{F} + \mathbf{S}$. When the lowest energy state is $|3, L_z\rangle$ or $|4, L_z\rangle$, the “dressed” spin of the impurity \mathbf{L} is antiparallel to the “bare” spin \mathbf{F} [see inequality (55)], and therefore we deal with over-screened Kondo effect.

Appendix H: $\text{Yb}(^3\text{P}_2)$ Atom in Magnetic Field

Appendices H and I main points: Although we do not subject our system to an external magnetic field (since it is detrimental for the Kondo effect) we find it useful to employ our detailed analysis of Yb atoms and inspect their properties under an application of a weak magnetic field. In particular, the multipole analysis worked out in this paper helps us to elucidate the pattern of the dependence of energy levels on the magnetic field, both for

the ground-state 1S_0 and the excited state 3P_2 . This is shown in Figs. 14(a), and 14(b).

Consider an 3P_2 Yb atom in external magnetic field. The Hamiltonian of the atom is,

$$\mathcal{H}_{\text{at}} = \mathcal{H}_{\text{at}}^{(0)} + \mathcal{H}_B, \quad (\text{H1})$$

where $\mathcal{H}_{\text{at}}^{(0)}$ is a Hamiltonian of the isolated ^{173}Yb atom in the 3P_2 state and \mathcal{H}_B describes interaction of the atom with the magnetic field,

$$\mathcal{H}_{\text{at}}^{(0)} = A_d \sum_{\alpha} \hat{I}^{\alpha} \hat{J}^{\alpha} + A_q \sum_{\alpha, \alpha'} \hat{I}^{\alpha, \alpha'} \hat{J}^{\alpha, \alpha'}, \quad (\text{H2})$$

$$\mathcal{H}_B = -g\mu_B B \hat{J}^z. \quad (\text{H3})$$

Here \hat{I}^{α} and $\hat{I}^{\alpha, \alpha'}$ are spin and quadrupole angular momentum operators for the nucleus, whereas J^{α} and $J^{\alpha, \alpha'}$ are orbital angular momentum and quadrupole angular momentum operators of the 3P_2 electronic configuration. g is the electronic g-factor of the Yb atom in the 3P_2 state, see eq. (70).

The constants A_d and A_q are³⁷,

$$\frac{A_d}{h} = -738 \text{ MHz}, \quad \frac{A_q}{h} = 1312 \text{ MHz}, \quad (\text{H4})$$

where h is the Planck constant, or

$$A_d = -3.052 \text{ } \mu\text{eV}, \quad A_q = 5.426 \text{ } \mu\text{eV}.$$

Taking into account definition (B2) for the quadrupole angular momentum operators, we can write the Hamiltonian (H2) in the form,

$$\begin{aligned} \mathcal{H}_{\text{at}}^{(0)} &= (A_d - 2A_q) (\hat{\mathbf{I}} \cdot \hat{\mathbf{J}}) + 4A_q (\hat{\mathbf{I}} \cdot \hat{\mathbf{J}})^2 - \\ &\quad - \frac{4}{3} A_q I(I+1)J(J+1). \end{aligned} \quad (\text{H5})$$

Eq. (H5) shows that eigenfunctions of $\mathcal{H}_{\text{at}}^{(0)}$ are also eigenfunctions of the operators $\hat{\mathbf{F}}^2$ and \hat{F}^z [where $\hat{\mathbf{F}} = \hat{\mathbf{I}} + \hat{\mathbf{J}}$ is the operator of the total atomic orbital momentum],

$$|F, f\rangle = \sum_{i,j} C_{I,i;J,j}^{F,f} |I, i; J, j\rangle, \quad (\text{H6})$$

where i , j and f are nuclear, electronic and total atomic magnetic quantum numbers. The wave functions $|I, i; J, j\rangle$ as eigenfunctions of the operators \hat{I}^z and \hat{J}^z ,

$$\begin{aligned} \hat{I}^z |I, i; J, j\rangle &= i |I, i; J, j\rangle, \\ \hat{J}^z |I, i; J, j\rangle &= j |I, i; J, j\rangle. \end{aligned}$$

Corresponding eigenenergies $\mathcal{E}_L^{(0)}$ are

$$\begin{aligned} \mathcal{E}_{\frac{1}{2}}^{(0)} &= -7A_d + 14A_q = 781.0 \text{ } \mu\text{eV}, \\ \mathcal{E}_{\frac{3}{2}}^{(0)} &= -\frac{11}{2} A_d + 62A_q = 353.2 \text{ } \mu\text{eV}, \\ \mathcal{E}_{\frac{5}{2}}^{(0)} &= -3A_d - 28A_q = -142.8 \text{ } \mu\text{eV}, \\ \mathcal{E}_{\frac{7}{2}}^{(0)} &= \frac{1}{2} A_d - 70 A_q = -381.3 \text{ } \mu\text{eV}, \\ \mathcal{E}_{\frac{9}{2}}^{(0)} &= 5 A_d + 20 A_q = 93.2 \text{ } \mu\text{eV}. \end{aligned}$$

The interaction Hamiltonian \mathcal{H}_B , eq. (H3), commutes with the operator \hat{F}^z , but not with $\hat{\mathbf{F}}^2$. Therefore, eigenfunctions of the Hamiltonian \mathcal{H}_{at} , eq. (H1), are described by the magnetic quantum numbers f , but not by the total atomic spin F .

In order to find eigenenergies of the Hamiltonian (H1), we find the matrix elements of \mathcal{H}_B ,

$$\begin{aligned} V_{F,F'}^{(f)} &= \langle F, f | \mathcal{H}_B | F', f \rangle = \\ &= -g\mu_B B C_{F,F'}^{(f)}, \end{aligned} \quad (\text{H7})$$

where

$$C_{F,F'}^{(f)} = \sum_{i,j} j C_{I,i;J,j}^{F,f} C_{I,i;J,j}^{F',f},$$

where $f = -\frac{9}{2}, -\frac{7}{2}, \dots, \frac{9}{2}$ and $f \leq F, F' \leq \frac{9}{2}$. Then the eigenenergies of \mathcal{H}_{at} are found from diagonalization of the matrices $\hat{h}^{(f)}$ with matrix elements $h_{F,F'}^{(f)}$ given by,

$$h_{F,F'}^{(f)} = \mathcal{E}_F^{(0)} \delta_{F,F'} + V_{F,F'}^{(f)}. \quad (\text{H8})$$

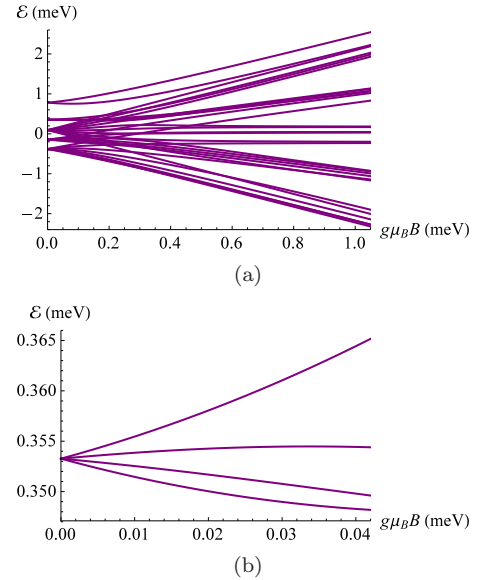


FIG. 14: (Color online) Energy spectrum of the ^{173}Yb atom in the 3P_2 quantum state [panel (a)]. Zeeman splitting of the $F = \frac{3}{2}$ energy level by a weak magnetic field [panel (b)].

The eigenvalues of the Hamiltonian (H1) as functions of the magnetic field are shown in Fig. 14(a). It is seen that for weak magnetic field [when $g\mu_B B$ is small with respect to the hyperfine splitting], every energy level $\mathcal{E}_F^{(0)}$ splits into $2F + 1$ spectral lines with energies $\mathcal{E}_{F,f}$ given by

$$\mathcal{E}_{F,f} = \mathcal{E}_F^{(0)} - g\mu_B B C_{F,F}^{(f)}. \quad (\text{H9})$$

For strong magnetic field [when $g\mu_B B$ is large with respect to the hyperfine splitting], the 3P_2 energy level

splits into 5 levels with $j_z = 0, \pm 1, \pm 2$, and every level splits into six levels by the hyperfine interaction.

Splitting of the $F = \frac{3}{2}$ energy level (that we are interested in) is,

$$\mathcal{E}_{\frac{3}{2},f} = \mathcal{E}_F^{(0)} - \frac{13}{30} g\mu_B B - f g\mu_B B. \quad (\text{H10})$$

Energies $\mathcal{E}_{\frac{3}{2},f}$ calculated numerically by diagonalization of the matrices (H8) are shown in Fig. 14(b) as functions of the magnetic field. The energies are almost linear with the magnetic field which agrees with equation (H10).

Appendix I: Averaged Dipole, Quadrupole and Octupole Moments

The density matrix of the impurity atom placed in the magnetic field $\mathbf{B} = B\mathbf{e}_z$ is,

$$\hat{\rho}_i = \frac{1}{Z_i} \sum_f e^{\beta g\mu_B B f} X^{f,f}, \quad (\text{I1})$$

where $\beta = \frac{1}{T}$,

$$Z_i = \sum_f e^{\beta g\mu_B B f}.$$

Expectation value of an operator \hat{O} acting in the Hilbert state of quantum states of the isolated impurity is,

$$\langle \hat{O} \rangle = \frac{1}{Z_i} \sum_f \mathcal{O}_{f,f},$$

where $\mathcal{O}_{f,f} = \langle f | \hat{O} | f \rangle$.

1. Expectation value of the magnetic dipole angular momentum operator is,

$$\langle \hat{F}^\alpha \rangle = -\mathcal{F}_d \delta^{\alpha,z}, \quad (\text{I2})$$

where

$$\mathcal{F}_d = \frac{1}{2} \tanh\left(\frac{g\mu_B B}{2T}\right) + \tanh\left(\frac{g\mu_B B}{T}\right).$$

When $g\mu_B B \ll T$, \mathcal{F}_d can be written in the linear with B approximation as,

$$\mathcal{F}_d = \frac{5}{4} \frac{g\mu_B B}{T} + O\left(\frac{\mu_B^3 B^3}{T^3}\right).$$

2. Expectation value of the magnetic quadrupole angular momentum operator is,

$$\langle \hat{F}^{\alpha,\alpha'} \rangle = -\mathcal{F}_q \delta^{\alpha,\alpha'} \left\{ \delta^{\alpha,x} + \delta^{\alpha,y} - 2\delta^{\alpha,z} \right\}, \quad (\text{I3})$$

where

$$\mathcal{F}_q = \frac{2 \sinh^2\left(\frac{g\mu_B B}{2T}\right)}{\cosh\left(\frac{g\mu_B B}{2T}\right)}.$$

When $g\mu_B B \ll T$, \mathcal{F}_q can be expanded with B as,

$$\mathcal{F}_q = \frac{1}{2} \frac{(g\mu_B B)^2}{T^2} + O\left(\frac{\mu_B^4 B^4}{T^4}\right).$$

3. Expectation value of the magnetic octupole angular momentum operator is,

$$\langle \hat{F}^{\alpha,\alpha',\alpha''} \rangle = \mathcal{F}_o \left\{ \delta^{\alpha,\alpha'} \delta^{\alpha'',z} + \delta^{\alpha,\alpha''} \delta^{\alpha',z} + \delta^{\alpha',\alpha''} \delta^{\alpha,z} - 5 \delta^{\alpha,z} \delta^{\alpha',z} \delta^{\alpha'',z} \right\}, \quad (\text{I4})$$

where

$$\mathcal{F}_o = \frac{36}{5} \frac{2 \sinh^4\left(\frac{g\mu_B B}{2T}\right)}{\sinh\left(\frac{2g\mu_B B}{2T}\right)}.$$

When $g\mu_B B \ll T$, \mathcal{F}_o can be expanded with B as,

$$\mathcal{F}_o = \frac{9}{40} \frac{(g\mu_B B)^3}{T^3} + O\left(\frac{\mu_B^5 B^5}{T^4}\right).$$

4. Expectation value of $F^{\alpha_1} F^{\alpha_2}$ is,

$$\frac{1}{2} \langle \hat{F}^{\alpha_1} \hat{F}^{\alpha_2} + \hat{F}^{\alpha_2} \hat{F}^{\alpha_1} \rangle = \left(\frac{5}{4} + \mathcal{F}_{d,d}^{\alpha_1} \right) \delta^{\alpha_1,\alpha_2}, \quad (\text{I5})$$

where

$$\mathcal{F}_{d,d}^\alpha = \left(3 \delta^{\alpha,z} - 1 \right) \frac{2 \sinh^2\left(\frac{g\mu_B B}{2T}\right)}{\cosh\left(\frac{g\mu_B B}{2T}\right)}.$$

When $g\mu_B B \ll T$, $\mathcal{F}_{d,d}$ can be expanded with B as,

$$\mathcal{F}_{d,d}^\alpha = \left(3 \delta^{\alpha,z} - 1 \right) \frac{1}{2} \frac{(g\mu_B B)^2}{T^2} + O\left(\frac{\mu_B^4 B^4}{T^4}\right).$$

5. Expectation value of $F^{\alpha_1} F^{\alpha_2, \alpha'_2}$ is,

$$\begin{aligned} \frac{1}{2} \langle \hat{F}^{\alpha_1} \hat{F}^{\alpha_2, \alpha'_2} + \hat{F}^{\alpha_2, \alpha'_2} \hat{F}^{\alpha_1} \rangle &= \\ &= \left(\delta^{\alpha_1, \alpha_2} \delta^{\alpha'_2, z} + \delta^{\alpha_1, \alpha'_2} \delta^{\alpha_2, z} - \right. \\ &\quad \left. - 2 \delta^{\alpha_1, z} \delta^{\alpha_2, z} \delta^{\alpha'_2, z} \right) \mathcal{F}_{d,q}^{(1)} + \\ &\quad + \delta^{\alpha_2, \alpha'_2} \left(\delta^{\alpha_1, z} - 2 \delta^{\alpha_1, z} \delta^{\alpha_2, z} \right) \mathcal{F}_{d,q}^{(2)}, \end{aligned} \quad (\text{I6})$$

where

$$\mathcal{F}_{d,q}^{(1)} = -\frac{3}{2} \tanh\left(\frac{g\mu_B B}{T}\right),$$

$$\mathcal{F}_{d,q}^{(2)} = \tanh\left(\frac{g\mu_B B}{2T}\right) - \frac{1}{2} \tanh\left(\frac{g\mu_B B}{T}\right).$$

When $g\mu_B B \ll T$, $\mathcal{F}_{d,q}^{(1,2)}$ can be expanded with B as,

$$\mathcal{F}_{d,q}^{(1)} = -\frac{3}{2} \frac{g\mu_B B}{T} + O\left(\frac{\mu_B^3 B^3}{T^3}\right),$$

$$\mathcal{F}_{d,q}^{(2)} = \frac{g\mu_B B}{T} + O\left(\frac{\mu_B^3 B^3}{T^3}\right).$$

6. Expectation value of $F^{\alpha_1} F^{\alpha_2, \alpha'_2, \alpha''_2}$ is,

$$\begin{aligned} & \frac{1}{2} \langle \hat{F}^{\alpha_1} \hat{F}^{\alpha_2, \alpha'_2, \alpha''_2} + \hat{F}^{\alpha_2, \alpha'_2, \alpha''_2} \hat{F}^{\alpha_1} \rangle = \\ & = \mathcal{A}^{\alpha_1; \alpha_2, \alpha'_2, \alpha''_2} \mathcal{F}_{d,o}, \end{aligned} \quad (I7)$$

where $\mathcal{A}^{\alpha_1; \alpha_2, \alpha'_2, \alpha''_2}$ is symmetric with $\alpha_2, \alpha'_2, \alpha''_2$ tensor which does not depend on temperature or magnetic field,

$$\mathcal{F}_{d,o} = \frac{2 \sinh^2 \left(\frac{g\mu_B B}{2T} \right)}{\cosh \left(\frac{g\mu_B B}{2T} \right)}.$$

When $g\mu_B B \ll T$, $\mathcal{F}_{d,o}$ can be expanded with B as,

$$\mathcal{F}_{d,o} = \frac{1}{2} \frac{(g\mu_B B)^2}{T^2} + O\left(\frac{\mu_B^4 B^4}{T^4}\right).$$

-
- ¹ J.Kondo, *Progr. Theor. Phys.* **32**, 37 (1964).
² P. Coleman, *Physics World* **12**, 29 (1995).
³ P. W. Anderson, *Physics World* **12**, 37 (1995).
⁴ A. C. Hewson, *The Kondo Problem to Heavy Fermions* (Cambridge University Press, Cambridge, 1993).
⁵ V. T. Rajan, *Phys. Rev. Lett.* **51**, 308 (1983).
⁶ P. Schlottmann, *Zeitschrift für Physik B: Condensed Matter* **51**, 223 (1983).
⁷ Andrés Jerez, Natan Andrei, and Gergely Zaránd, *Phys. Rev. B* **58**, 3814 (1998).
⁸ P. Nozières and A. Blandin, *J. Phys. (Paris)* **41**, 193 (1980).
⁹ Y. Oreg and D. Goldhaber-Gordon, *Phys. Rev. Lett.* **90**, 136602 (2003).
¹⁰ A. M. Sengupta and Y. B. Kim, *Phys. Rev. B* **54**, 14918 (1996).
¹¹ C. Silber, S. Gunther, C. Marzok, B. Deh, P. W. Courteille, and C. Zimmermann, *Phys. Rev. Lett.* **95**, 170408 (2005).
¹² T. Onimaru, K. Izawa, K. T. Matsumoto, T. Yoshida, Y. Machida, T. Ikeura, K. Wakiya, K. Umeo, S. Kittaka, K. Araki, T. Sakakibara, T. Takabatake, *Phys. Rev. B* **94**, 075134 (2016); arXiv:1606.09571.
¹³ I. Kuzmenko, T. Kuzmenko, Y. Avishai and K. A. Kikoin, *Phys. Rev. B* **91**, 165131 (2015); arXiv:1402.0187.
¹⁴ Olivier Parcollet, Antoine Georges, Gabriel Kotliar, and Anirvan Sengupta, *Phys. Rev. B* **58**, 3794 (1998); arXiv:cond-mat/9711192.
¹⁵ T.Fukuhara, Y.Takasu, M.Kumakura, Y.Takahashi, *Phys. Rev. Lett.* **98**, 030401 (2007).
¹⁶ Ren Zhang, Yanting Cheng, Hui Zhai, Peng Zhang, *Phys. Rev. Lett.* **115**, 135301 (2015); arXiv:1504.02864.
¹⁷ Luis Riegger, Nelson Darkwah Oppong, Moritz Höfer, Diogo Rio Fernandes, Immanuel Bloch, Simon Fölling, arXiv:1708.03810 (2017)
¹⁸ Ren Zhang, Deping Zhang, Yanting Cheng, Wei Chen, Peng Zhang, Hui Zhai, *Phys. Rev. A* **93**, 043601 (2016); arXiv:1509.01350.
¹⁹ G. Pagano, M. Mancini, G. Cappellini, L. Livi, C. Sias, J. Catani, M. Inguscio, and L. Fallani, *Phys. Rev. Lett.* **115**, 265301 (2015).
²⁰ Guido Pagano, Marco Mancini, Giacomo Cappellini, Pietro Lombardi, Florian Schäfer, Hui Hu, Xia-Ji Liu, Jacopo Catani, Carlo Sias, Massimo Inguscio and Leonardo Fallani, *Nature Physics* **10**, 198 (2014).
²¹ Giacomo Cappellini, Marco Mancini, Guido Pagano, Pietro Lombardi, Lorenzo Livi, Mario Siciliani de Cumis, Pablo Cancio, Marco Pizzocaro, Davide Calonico, Filippo Levi, Carlo Sias, Jacopo Catani, Massimo Inguscio, Leonardo Fallani, *Phys. Rev. Lett.* **113**, 120402 (2014).
²² F. Scazza, C. Hofrichter, M. Höfer, P. C. De Groot, I. Bloch, and S. Fölling, *Nature Physics* **10**, 779 (2014).
²³ T. D. Ladd, F. Jelezko, R. Laflamme, Y. Nakamura, C. Monroe, and J. L. O'Brien, *Nature* **464**, 45 (2010).
²⁴ A. J. Daley, *Quantum Information Processing* **10**, 865 (2011).
²⁵ X. Zhang, M. Bishof, S. L. Bromley, C. V. Kraus, M. S. Safronova, P. Zoller, A. M. Rey, and J. Ye, *Science* **345**, 1467 (2014).
²⁶ B. Song, C. He, S. Zhang, E. Hajiyev, W. Huang, X.-J. Liu, and G.-B. Jo, *Physical Review A Rapid Communications* **94**, 061604(R) (2016).
²⁷ S. Kolkowitz, S. L. Bromley, T. Bothwell, M. L. Wall, G. E. Marti, A. P. Koller, X. Zhang, A. M. Rey, and J. Ye, *Nature* **542**, 6670 (2017).
²⁸ L. F. Livi, G. Cappellini, M. Diem, L. Franchi, C. Clivati, M. Frittelli, F. Levi, D. Calonico, J. Catani, M. Inguscio, L. Fallani, arXiv:1609.04800.
²⁹ Bo Song, Long Zhang, Chengdong He, Ting Fung Jeffrey Poon, Elnur Hajiyev, Shanchao Zhang, Xiong-Jun Liu and Gyu-Boong Jo, arXiv:1706.00768 (2017).
³⁰ S.L. Bromley, S. Kolkowitz, T. Bothwell, D. Kedar, A. Safavi-Naini, M.L. Wall, C. Salomon, A.M. Rey, J. Ye, arXiv:1708.02704 (2017).
³¹ A. Yamaguchi, S. Uetake, S. Kato, H. Ito, and Y. Takahashi, *New Journal of Physics* **12**, 103001 (2010).
³² A. Khramov, A. Hansen, W. Dowd, R. J. Roy, C. Makrides, A. Petrov, S. Kotochigova, and S. Gupta, *Physical Rev. Lett.* **112**, 033201 (2014).
³³ Igor Kuzmenko, Tetyana Kuzmenko, Yshai Avishai, Gyu-Boong Jo, *Phys. Rev. B* **93**, 115143 (2016); arXiv:1512.00978.
³⁴ G. F. Gribakin and V. V. Flambaum, *Phys. Rev. A* **48**, 546 (1993).
³⁵ Masaaki Kitagawa, Katsunari Enomoto, Kentaro Kasa, Yoshiro Takahashi, Roman Ciurylo, Pascal Naidon, and Paul S. Julienne, *Phys. Rev. A* **77**, 012719 (2008); arXiv:0708.0752.
³⁶ L. D. Landau and E. M. Lifshitz, *Quantum Mechanics, A Course of Theoretical Physics Vol. 3* (Pergamon, New York, 1965).
³⁷ S.G. Porsev, Yu.G. Rakhlina, M.G. Kozlov, *J. Phys. B* **32**, 1113-20 (1999); arXiv:physics/9810011.
³⁸ Masses, nuclear spins, and magnetic moments: I. Mills, T. Cvitas, K. Homann, N. Kallay, and K. Kuchitsu, in *Quantities, Units and Symbols in Physical Chemistry*, Blackwell Scientific Publications, Oxford, UK, 1988.
³⁹ S.G. Porsev, M.S. Safronova, A. Derevianko, Charles W. Clark, *Phys. Rev. A* **89**, 012711 (2014); arXiv:1307.2656 .
⁴⁰ W. F. Meggers and J. L. Tech, *J. Res. Natl. Bur. Stand. (U.S.)* **83**, 13 (1978).
⁴¹ T. Andersen, "Atomic negative ions: Structure, dynamics

- and collisions". *Physics Reports* **394**, 157 (2004).
- ⁴² Shinya Kato, Seiji Sugawa, Kosuke Shibata, Ryuta Yamamoto, and Yoshiro Takahashi, *Phys. Rev. Lett.* **110**, 173201 (2013); arXiv:1210.2483.
- ⁴³ Nir Navon, Swann Piatecki, Kenneth Günter, Benno Rem, Trong Canh Nguyen, Frédéric Chevy, Werner Krauth, and Christophe Salomon, *Phys. Rev. Lett.* **107**, 135301 (2011).
- ⁴⁴ Nascimbène, S and Navon, N and Jiang, K J and Chevy, F. and SALOMON, C, *Nature* **463**, 1057 (2010)
- ⁴⁵ Hofrichter, Christian and Riegger, Luis and Scazza, Francesco and Höfer, Moritz and Fernandes, Diogo Rio and Bloch, Immanuel and Fölling, Simon, *Physical Review X*, **6**, 021030 (2016)
- ⁴⁶ Qi Zhou and T.-L. Ho, *Nature Physics*, **6**(2), 131 (2009)
- ⁴⁷ G. Valtolina, F. Scazza, A. Amico, A. Burchianti, A. Recati, T. Enss, M. Inguscio, M. Zaccanti, G. Roati, arXiv:1605.07850 (2016)
- ⁴⁸ Sanner, Christian and Su, Edward J and Keshet, Aviv and Huang, Wujie and Gillen, Jonathon and Gommers, Ralf and Ketterle, Wolfgang, *Physical Review Letters* **106** 010402 (2011)
- ⁴⁹ Y.R. Lee, T.T. Wang, T.M. Rvachov, J.H. Choi, W. Ketterle, and M.-S. Heo, *Phys. Rev. A* **87**, 043629 (2013)
- ⁵⁰ Mark J. H. Ku, Ariel T. Sommer, Lawrence W. Cheuk, Martin W. Zwierlein, *Science* **335**, 563 (2012).